Models of the Pseudogap State of Two-Dimensional Systems

E.Z.Kuchinskii, M.V.Sadovskii
Institute for Electrophysics,
Russian Academy of Sciences, Ural Branch,
Ekaterinburg 620049, Russia
E-mail: kuchinsk@ief.uran.ru, sadovski@ief.uran.ru

Abstract

We analyze a number of "nearly exactly" solvable models of electronic spectrum of two-dimensional systems with well-developed fluctuations of short range order of "dielectric" (e.g. antiferromagnetic) or "superconducting" type, which lead to the formation of anisotropic pseudogap state on certain parts of the Fermi surface. We formulate a recurrence procedure to calculate one-electron Green's function which takes into account all Feynman diagrams in perturbation series and is based upon the approximate Ansatz for higher-order terms in this series. Detailed results for spectral densities and density of states are presented. We also discuss some important points concerning the justification of our Ansatz for higher-order contributions.

PACS numbers: 74.20.Mn, 74.72.-h, 74.25.-q, 74.25.Jb

Contents

I. INTRODUCTION.

Recently there was an upsurge of interest in observation of the pseudogap in the spectrum of elementary excitations of underdoped high-temperature superconductors (HTSC) [1,2]. These anomalies were observed in a number of experiments, such as the measurements of optical conductivity, NMR, inelastic neutron scattering and angle-resolved photoemission (ARPES) (cf. review in [1]). Probably most striking evidence for the existence of this unusual state were obtained in ARPES–experiments [3,4], which demonstrated essentially anisotropic changes in the spectral density of current carriers in rather wide temperature region in normal (nonsuperconducting) phase of these systems (cf. review in [2]). A remarkable anomaly observed in these experiments was that the most significant changes (in comparison with the usual Fermi-liquid behavior) in spectral density were seen close to the point $(\pi, 0)$ in the Brillouin zone, while there were no changes at all in the direction of zone diagonal (point (π, π)), which in fact demonstrates the "destruction" of the Fermi surface around the point $(\pi, 0)$ and conservation of Fermi–liquid behavior in the direction of zone diagonal. In this sense it is usually claimed that the pseudogap symmetry is of the "d-wave" type, the same as the symmetry of superconducting energy gap in these compounds [1,2]. At the same time the mere fact that these anomalies exist at the temperatures much higher than superconducting transition temperature, as well as in the underdoped (non optimal) region of carrier concentrations, may signify some other nature of these anomalies, not connected directly with Cooper pairing. Typical phase diagram of HTSC–system is shown in Fig.1.

There are rather many theoretical papers now attempting to interpret the observed anomalies. We may classify these attempts in two main schools of thought (scenarios). One is based upon the idea of Cooper pairs (fluctuation) formation at temperatures higher than the usual superconducting transition temperature [1,5–7]. Another assumes that the pseudogap phenomena are determined mainly by fluctuations of antiferromagnetic (AFM) short range order [8–12].

Rather long ago one of the authors of the present paper had proposed an exactly solvable model of the pseudogap formation in one-dimensional system due to well developed fluctuations of short range order of charge density (CDW) or spin density (SDW) wave [13–17]. Recently this model has attracted some interest in connection with attempts to understand the pseudogap state in HTSC-cuprates [11,12,18–20]. In particular in Refs. [11,12] an important generalization of this model was formulated for the case of two-dimensional electronic system with random field of spin fluctuations (AFM short range order). In this model of "hot spots" on the Fermi surface [11,12], using the formal scheme of Refs. [15–17], they obtained rather detailed description of pseudogap anomalies for the case of large enough temperatures ("weak pseudogap" region in Fig.1). In Refs. [19,20] a simplified variant of this model [13,14], corresponding to the limit of very large correlation lengths of fluctuations of short range order, was used to describe the pseudogap state determined by well developed fluctuations of superconducting (SC) short range order. In a recent paper [21] this (over) simplified model was used to derive Ginzburg–Landau expansion (for different types of Cooper pairing) for the system with strong fluctuations of CDW(SDW,AFM)–type, in the framework of "hot patches" model proposed in this work. At the same time, in Ref. [22], dedicated to rather detailed review of the model proposed in Refs. [13–17], a certain error

was noted in early papers [15–17] in the analysis of the case of finite correlation lengths of fluctuations of short range order. In Ref. [12] it was claimed that this error is rather insignificant, especially in two- dimensional model of "hot spots", which is of the main interest for the physics of HTSC-cuprates.

The aim of the present paper is to perform an analysis of number of important aspects of this "nearly exactly" solvable model, mainly for two-dimensional case. We shall consider both the case of short range order fluctuations of CDW(SDW,AFM)–type in the "hot spots " model [11,12], as well as the possible applications of this model in the scenario of superconducting fluctuations [7,19,20] (SC short range order), in particular for the most interesting case of d-wave pairing. Besides the general discussion of reliability of the formal scheme of Refs. [13–17,11,12], we shall perform detailed calculations of the spectral densities and one-electron density of states both for the "hot spots" model [11,12], and in the scenario of SC–fluctuations.

II. "HOT–SPOTS" MODEL.

1. Model description and "nearly exact" solution for the Green's function.

The model of "nearly-antiferromagnetic" Fermi-liquid [23,24] is based upon the picture of well developed fluctuations of AFM short range order in a wide region of phase diagram shown in Fig.1. In this model the effective interaction of electrons with spin fluctuations is described via dynamic spin susceptibility $\chi_{\mathbf{q}}(\omega)$, which is determined mainly from the fit to NMR experiments [24]:

$$V_{eff}(\mathbf{q},\omega) = g^2\chi_{\mathbf{q}}(\omega) \approx \frac{g^2\xi^2}{1+\xi^2(\mathbf{q}-\mathbf{Q})^2 - i\frac{\omega}{\omega_{sf}}} \tag{1}$$

where g is coupling constant, ξ–correlation length of spin fluctuations, $\mathbf{Q} = (\pi/a, \pi/a)$–vector of antiferromagnetic ordering in insulating phase, ω_{sf}–characteristic frequency of spin fluctuations, a–lattice spacing.

As dynamic spin susceptibility $\chi_{\mathbf{q}}(\omega)$ has peaks at the wave vectors around $(\pi/a, \pi/a)$ there appear "two types" of quasiparticles —"hot quasiparticles" with momenta in the vicinity of "hot spots" on the Fermi surface (Fig.2) and "cold" quasiparticles with momenta on the other parts of the Fermi surface, e.g. around diagonals of the Brillouin zone $|p_x| = |p_y|$ [11,12]. These terms are connected with the fact that quasiparticles from the vicinity of "hot spots" are strongly scattered on the vector of the order of $\mathbf{Q}$ by spin fluctuations (1), while for quasiparticles with momenta far from "hot spots" this interaction is relatively weak.

In the following we shall consider the case of high enough temperatures when $\pi T \gg \omega_{sf}$ which corresponds to the region of "weak pseudogap" in Fig.1 [11,12]. In this case spin dynamics is irrelevant and we can limit ourselves to static approximation:

$$V_{eff}(\mathbf{q}) = \tilde{\Delta}^2\frac{\xi^2}{1+\xi^2(\mathbf{q}-\mathbf{Q})^2} \tag{2}$$

where $\tilde{\Delta}$–effective energy parameter, which in the model of AFM fluctuations can be written as [12]:

$$\tilde{\Delta}^2 = g^2 T \sum_{m\mathbf{q}} \chi_{\mathbf{q}}(i\omega_m) = g^2 < \mathbf{S}_i^2 > /3 \tag{3}$$

where $\mathbf{S}_i$–spin on the lattice site (Cu ion in highly conducting CuO_2–plane for HTSC-cuprates). In the following we shall consider $\tilde{\Delta}$ (as well as ξ) as some phenomenological parameter, determining the effective width of the pseudogap.

We can greatly simplify all calculations if instead of (2) we use another form of model interaction (cf. analogous model in [8]):

$$V_{eff}(\mathbf{q}) = \Delta^2 \frac{2\xi^{-1}}{\xi^{-2} + (q_x - Q_x)^2} \frac{2\xi^{-1}}{\xi^{-2} + (q_y - Q_y)^2} \tag{4}$$

where $\Delta^2 = \tilde{\Delta}^2/4$. In fact (4) is qualitatively similar to (2) and differs from it very slightly in most important region of $|\mathbf{q} - \mathbf{Q}| < \xi^{-1}$.

Consider the first order in V_{eff} correction to electron self-energy shown in Fig.3:

$$\Sigma(\varepsilon_n \mathbf{p}) = \sum_{\mathbf{q}} V_{eff}(\mathbf{q}) \frac{1}{i\varepsilon_n - \xi_{\mathbf{p}+\mathbf{q}}} \tag{5}$$

Main contribution to the sum over $\mathbf{q}$ comes from the region close to $\mathbf{Q} = (\pi/a, \pi/a)$. Then we can write:

$$\xi_{\mathbf{p}+\mathbf{q}} = \xi_{\mathbf{p}+\mathbf{Q}+\mathbf{k}} \approx \xi_{\mathbf{p}+\mathbf{Q}} + \mathbf{v}_{\mathbf{p}+\mathbf{Q}}\mathbf{k} \tag{6}$$

where $v^{\alpha}_{\mathbf{p}+\mathbf{Q}} = \frac{\partial \xi_{\mathbf{p}+\mathbf{Q}}}{\partial p_\alpha}$, and performing integration over $\mathbf{k}$, we get: [1]

$$\Sigma(\varepsilon_n \mathbf{p}) = \frac{\Delta^2}{i\varepsilon_n - \xi_{\mathbf{p}+\mathbf{Q}} + (|v^x_{\mathbf{p}+\mathbf{Q}}| + |v^y_{\mathbf{p}+\mathbf{Q}}|)\kappa sign\varepsilon_n} \tag{7}$$

where $\kappa = \xi^{-1}$.

The spectrum of "bare" (free) quasiparticles can be taken in the form [11,12]:

$$\xi_{\mathbf{p}} = -2t(\cos p_x a + \cos p_y a) - 4t' \cos p_x a \cos p_y a \tag{8}$$

where t–nearest neighbor transfer integral, t'–second nearest neighbor transfer integral on the square lattice, μ is chemical potential. In the analysis of real HTSC-systems in Refs. [11,12] it was assumed e.g. for $YBa_2Cu_3O_{6+\delta}$ that $t = 0.25eV$, $t' = -0.45t$, while μ was fixed by hole concentration. Below we shall see that it is of considerable interest to study our problem for different relations between t and t'.

---

[1] In Refs. [11,12] another but similar in spirit to (4) form of effective interaction was used: $V_{eff}(\mathbf{k}) = \boldsymbol{\Delta}^2 \frac{2\xi^{-1}}{\xi^{-2}+\mathbf{k}_\parallel^2} \frac{2\xi^{-1}}{\xi^{-2}+\mathbf{k}_\perp^2}$, where $k_{\parallel(\perp)}$ –projection of $\mathbf{k}$ parallel (perpendicular) to $\mathbf{v}_{\mathbf{p}+\mathbf{Q}}$, so that result analogous to (7) takes the form:

$$\Sigma(\varepsilon_n \mathbf{p}) = \frac{\Delta^2}{i\varepsilon - \xi_{\mathbf{p}+\mathbf{Q}} + i|\mathbf{v}_{\mathbf{p}+\mathbf{Q}}|\kappa sign\varepsilon_n}$$

Consider second order corrections to self-energy shown in Fig.4. Using (4) we obtain:

$$\Sigma(a) = \Delta^4 \int \frac{d\mathbf{k_1}}{\pi^2} \int \frac{d\mathbf{k_2}}{\pi^2} \frac{\kappa}{\kappa^2+k_{1x}^2} \frac{\kappa}{\kappa^2+k_{1y}^2} \frac{\kappa}{\kappa^2+k_{2x}^2} \frac{\kappa}{\kappa^2+k_{2y}^2}$$
$$\frac{1}{i\varepsilon_n - \xi_{\mathbf{p+Q}} - v^x_{\mathbf{p+Q}} k_{1x} - v^y_{\mathbf{p+Q}} k_{1y}} \frac{1}{i\varepsilon_n - \xi_{\mathbf{p}} - v^x_{\mathbf{p}}(k_{1x}+k_{2x}) - v^y_{\mathbf{p}}(k_{1y}+k_{2y})}$$
$$\frac{1}{i\varepsilon_n - \xi_{\mathbf{p+Q}} - v^x_{\mathbf{p+Q}} k_{1x} - v^y_{\mathbf{p+Q}} k_{1y}} \tag{9}$$

$$\Sigma(b) = \Delta^4 \int \frac{d\mathbf{k_1}}{\pi^2} \int \frac{d\mathbf{k_2}}{\pi^2} \frac{\kappa}{\kappa^2+k_{1x}^2} \frac{\kappa}{\kappa^2+k_{1y}^2} \frac{\kappa}{\kappa^2+k_{2x}^2} \frac{\kappa}{\kappa^2+k_{2y}^2}$$
$$\frac{1}{i\varepsilon_n - \xi_{\mathbf{p+Q}} - v^x_{\mathbf{p+Q}} k_{1x} - v^y_{\mathbf{p+Q}} k_{1y}} \frac{1}{i\varepsilon_n - \xi_{\mathbf{p}} - v^x_{\mathbf{p}}(k_{1x}+k_{2x}) - v^y_{\mathbf{p}}(k_{1y}+k_{2y})}$$
$$\frac{1}{i\varepsilon_n - \xi_{\mathbf{p+Q}} - v^x_{\mathbf{p+Q}} k_{2x} - v^y_{\mathbf{p+Q}} k_{2y}} \tag{10}$$

where we have used the spectrum (8), from which, in particular, it follows that $\xi_{\mathbf{p+2Q}} = \xi_{\mathbf{p}}$, $\mathbf{v_{p+2Q}} = \mathbf{v_p}$ for $\mathbf{Q} = (\pi/a, \pi/a)$. If signs of $v^x_{\mathbf{p}}$ and $v^x_{\mathbf{p+Q}}$, and of $v^y_{\mathbf{p}}$ and $v^y_{\mathbf{p+Q}}$ are the same, we can see that integrals in (9) and (10) are fully determined by poles of Lorentzians, which determine the interaction with fluctuations. After elementary contour integration we obtain: [2]

$$\Sigma(a) = \Sigma(b) = \frac{1}{[i\varepsilon_n - \xi_{\mathbf{p+Q}} + i(|v^x_{\mathbf{p+Q}}| + |v^y_{\mathbf{p+Q}}|)\kappa]^2} \frac{1}{i\varepsilon_n - \xi_{\mathbf{p}} + i2(|v^x_{\mathbf{p}}| + |v^y_{\mathbf{p}}|)\kappa} \tag{11}$$

Here and in the following we assume $\varepsilon_n > 0$. It is easy to convince ourselves that in case of velocity projections of the same sign we can similarly calculate contributions of any higher order diagrams. Accordingly, the contribution of an arbitrary diagram for electron self-energy of N-th order in interaction (4) has the form:

$$\Sigma^{(N)}(\varepsilon_n \mathbf{p}) = \Delta^{2N} \prod_{j=1}^{2N-1} \frac{1}{i\varepsilon_n - \xi_j + i n_j v_j \kappa} \tag{12}$$

where $\xi_j = \xi_{\mathbf{p+Q}}$ and $v_j = |v^x_{\mathbf{p+Q}}| + |v^y_{\mathbf{p+Q}}|$ for odd j and $\xi_j = \xi_{\mathbf{p}}$ and $v_j = |v^x_{\mathbf{p}}| + |v^y_{\mathbf{p}}|$ for even j. Here n_j is the number of interaction lines, enveloping j-th Green's function in a given diagram.

In this case any diagram with intersecting interaction lines is actually equal to some diagram of the same order with noncrossing interaction lines. Thus in fact we can consider

---

[2] In the model of V_{eff} used in Ref. [11,12], for the case of $\mathbf{v_p v_{p+Q}} > 0$, in a similar way we get:

$$\Sigma(a) = \Sigma(b) = \Delta^4 \frac{1}{[i\varepsilon_n - \xi_{\mathbf{p+Q}} + i|\mathbf{v_{p+Q}}|\kappa]^2} \frac{1}{i\varepsilon_n - \xi_{\mathbf{p+Q}} + i2|\mathbf{v_p}|(|\cos\phi| + |\sin\phi|)\kappa}$$

where ϕ–angle between $\mathbf{v_p}$ and $\mathbf{v_{p+Q}}$.

only diagrams with nonintersecting interaction lines, taking into account diagrams with intersecting lines introducing additional combinatorial factors into interaction vertices. This method was first introduced (for another problem) in a paper by Elyutin [25] and used for one-dimensional model of the pseudogap state in Refs. [15–17].

As a result we obtain the following recursion relation for one-electron Green's function (continuous fraction representation) [15–17]):

$$G^{-1}(\varepsilon_n \xi_{\mathbf{p}}) = G_0^{-1}(\varepsilon_n \xi_{\mathbf{p}}) - \Sigma_1(\varepsilon_n \xi_{\mathbf{p}}) \tag{13}$$

$$\Sigma_k(\varepsilon_n \xi_{\mathbf{p}}) = \Delta^2 \frac{v(k)}{i\varepsilon_n - \xi_k + ikv_k\kappa - \Sigma_{k+1}(\varepsilon_n \xi_{\mathbf{p}})} \tag{14}$$

where $\xi_k = \xi_{\mathbf{p+Q}}$ and $v_k = |v^x_{\mathbf{p+Q}}| + |v^y_{\mathbf{p+Q}}|$ for odd values of k, $\xi_k = \xi_{\mathbf{p}}$ and $v_k = |v^x_{\mathbf{p}}| + |v^y_{\mathbf{p}}|$ for even k. Combinatorial factor:

$$v(k) = k \tag{15}$$

corresponds to our case of commensurate fluctuations with $\mathbf{Q} = (\pi/a, \pi/a)$ [15]. It is not difficult to analyze also the case of incommensurate fluctuations when $\mathbf{Q}$ is not "locked" to the period of inverse lattice. In this case diagrams with interaction lines enveloping odd number of vertices are significantly smaller than diagrams with interaction lines enveloping even number of vertices. Thus we must consider only these last diagrams [13–17]. Recurrence relation has the same form (14), but diagram combinatorics and factors $v(k)$ change [15]:

$$v(k) = \begin{cases} \frac{k+1}{2} & \text{for odd } k \\ \frac{k}{2} & \text{for even } k \end{cases} \tag{16}$$

In Refs. [11,12] a spin-structure of effective interaction within the model of "nearly antiferromagnetic" Fermi-liquid was taken into account (spin-fermion model of Ref. [12]). This leads to more complicated combinatorics of diagrams in the commensurate case with $\mathbf{Q} = (\pi/a, \pi/a)$. Spin-conserving part of the interaction gives formally commensurate combinatorics, while spin-flip scattering is described by diagrams with combinatorics of incommensurate type ("charged" random field in terms of Ref. [12]). As a result the recurrence relation for the Green's function is again of the form of(14), but the combinatorial factor $v(k)$ is now [11,12]:

$$v(k) = \begin{cases} \frac{k+2}{3} & \text{for odd } k \\ \frac{k}{3} & \text{for even } k \end{cases} \tag{17}$$

As we noted above, the solution of the form of (14) can be obtained only in the case of coinciding signs of velocity projections $v^x_{\mathbf{p+Q}}(v^y_{\mathbf{p+Q}})$ and $v^x_{\mathbf{p}}(v^y_{\mathbf{p}})$. Below we shall analyze situations when this is really so. In case of different signs of these projections integrals of the type of (9) and (10), corresponding to higher order corrections, can not be calculated in such a simple way as above, because contributions from the poles of the Green's functions become relevant. In this case, instead of simple answers like (11) rather cumbersome expressions appear and, even more importantly, disappears the fundamental (for our method) fact of equality of wide range of diagrams with crossing and noncrossing interaction lines, which

actually allows us to classify higher order contributions and obtain an "exact" solution (14). This problem is important only for the case of finite correlation lengths of fluctuations $\xi = \kappa^{-1}$, while in the limit of $\xi \to \infty(\kappa \to 0)$ the exact solution for the Green's function is independent of velocities $\mathbf{v_p}$ and $\mathbf{v_{p+Q}}$ and can be easily obtained in analytic form by methods of Refs. [13,14] (cf. also [12]). In one-dimensional model considered in Refs. [13–17] the signs of corresponding velocity projections are always different (these correspond to "left" and "right" moving electrons). This problem was stressed in a recent paper [22]. In Appendix A we analyze these difficulties in detail for one-dimensional case and show that the "Ansatz" of the type of (12) used in Refs. [15–17] for the contributions of higher order diagrams as well as solution of the form of (14) in fact give us very good approximation to an exact solution even in the case of velocity projections of different signs. Obviously this solution is exact in the limits of $\xi \to \infty(\kappa \to 0)$ and $\xi \to 0(\kappa \to \infty)$, and guarantees rather good (qualitatively) description in the region of finite correlation lengths.

2. Analysis of the "bare" energy-spectrum.

For the "bare" energy spectrum (8) we can easily find conditions (relations between t,t' and μ), when solution (14) is exact. First of all, let us define the region of parameters t,t' and μ, when "hot spots" on the Fermi surface exist, i.e. the condition of existence of points connected with vector $\mathbf{Q} = (\pi/a, \pi/a)$. If $\mathbf{p} = (p_x, p_y)$ is the position of a "hot spot" on the Fermi surface, then $\mathbf{p} + \mathbf{Q} = (p_x + \pi/a, p_y + \pi/a)$ must also belong to the Fermi surface, so that for the spectrum (8) we must have:

$$\begin{aligned} -2t(\cos p_x a + \cos p_y a) - 4t' \cos p_x a \cos p_y a - \mu = 0 \\ 2t(\cos p_x a + \cos p_y a) - 4t' \cos p_x a \cos p_y a - \mu = 0 \end{aligned} \tag{18}$$

Then the condition of existence of "hot spots" becomes:

$$\cos p_y a = -\cos p_x a \qquad \text{and} \qquad \cos^2 p_x a = \frac{\mu}{4t'} \tag{19}$$

Thus, the "hot spots" on the Fermi surface exist if:

$$0 \le \frac{\mu}{4t'} \le 1 \tag{20}$$

Define now the region of parameters t,t' and μ where (14) is exact requiring the positivity of products $v^x_{\mathbf{p}} v^x_{\mathbf{p+Q}}$ and $v^y_{\mathbf{p}} v^y_{\mathbf{p+Q}}$. We have:

$$\begin{aligned} v^x_{\mathbf{p}} &= \frac{\partial \xi_{\mathbf{p}}}{\partial p_x} = 2t \sin p_x a + 4t' \sin p_x a \cos p_y a \\ v^y_{\mathbf{p}} &= \frac{\partial \xi_{\mathbf{p}}}{\partial p_y} = 2t \sin p_y a + 4t' \sin p_y a \cos p_x a \\ v^x_{\mathbf{p}} v^x_{\mathbf{p+Q}} &= 16t'^2 \sin^2 p_x a [\cos^2 p_y a - (\frac{t}{2t'})^2] \\ v^y_{\mathbf{p}} v^y_{\mathbf{p+Q}} &= 16t'^2 \sin^2 p_y a [\cos^2 p_x a - (\frac{t}{2t'})^2] \end{aligned} \tag{21}$$

It is easily seen that for the existence of points on the Fermi surface, where the projections of velocities are of the same signs, it is necessary to fulfil $|t'/t| > 1/2$. We are mainly interested in the region around the "hot spots", where with an account of(19) we have:

$$v^x_{\mathbf{p}} v^x_{\mathbf{p+Q}} = v^y_{\mathbf{p}} v^y_{\mathbf{p+Q}} = 4t^2(1 - \frac{\mu}{4t'})(\frac{\mu t'}{t^2} - 1) \tag{22}$$

Thus the projections of velocities in "hot spots" have the same sign if:

$$\frac{\mu t'}{t^2} > 1 \tag{23}$$

The same condition obviously guarantees the validity of inequality $\mathbf{v_p v_{p+Q}} > 0$ which is necessary for exactness of (14) in the model of Refs. [11,12].

In Fig.5 we show (dashed region) the region of parameters where "hot spots" exist ($0 \leq \mu/4t' \leq 1$) as well as the region where velocity projections in their vicinity are of the same sign ($\mu t' > 1$). In Fig.6 we show the Fermi surfaces, defined by the "bare" spectrum (8), for different values of chemical potential μ (band fillings) when these conditions are either satisfied or not.

3. Spectral density and density of states.

Consider one-electron spectral density:

$$A(E\mathbf{p}) = -\frac{1}{\pi} Im G^R(E\mathbf{p}) \tag{24}$$

where $G^R(E\mathbf{p})$ is retarded Green's function, obtained by the usual analytic continuation of (13) to the real axis of energy E. In Fig.7 we show energy dependencies of $A(E\mathbf{p})$ obtained from (13),(14) for different variants of combinatorial factors (15),(16),(17). For $t'/t = -0.6$ and $\mu/t = -1.8 < t/t' = 1.666$ projections of velocities in "hot spots" are of the same sign and relation (14) defines Green's function exactly. We can see that in incommensurate case (16) (Fig.7(a)) as well as for combinatorics of spin-fermion model (17) (Fig.7(c)) the spectral density at the "hot spot" demonstrates clearly non Fermi-liquid behavior (for large enough values of correlation length ξ). Note also that for both cases the numerical values of spectral density are very close. In the case of commensurate combinatorics (15) (Fig.7(b)) precisely at the "hot spot" the spectral density has a single peak and, in this sense, is similar to that of the Fermi-liquid even for large values of ξ. However, even in the nearest neighborhood of "hot spot" this spectral density acquires two peak structure ("shadow" band) of non Fermi-liquid type for large enough values of ξ (see insert in Fig.7(b)).

Far from "hot spots" velocity projections are, in general, of different signs even if condition (23) is satisfied. Accordingly, the recurrence relation (14) for the Green's function is non exact here. [3] However, from discussion in Appendix A it becomes clear that our

---

[3] At the same time, with the growth of ξ more narrow vicinity of the "hot spot" becomes important and our approximation is more and more accurate.

"Ansatz" (12) and solution (14) in fact somehow overestimate the role of finite correlation length ξ. There we also provide slightly different variant of solution (A11), which somehow underestimates this role. Inserts in Fig.7 we show energy dependencies of spectral density far from the "hot spot" for different combinatorics of diagrams (15), (16), (17).

For comparison we also show the spectral density (for incommensurate case) obtained with an "Ansatz of alternating κ"(A11) which happens to be very close to that obtained from (13), (14). This confirms rather high accuracy of (14) for arbitrary momenta close to the Fermi surface.

In Fig.8 we show energy dependencies of spectral density for different combinatorics (15),(16),(17) at the "hot spot" in the case of $t'/t = -0.4$, which, according to Ref. [11,12], corresponds to $YBa_2Cu_3O_{6+\delta}$. For this value of t/t' even at the "hot spot" velocity projections are of different signs. However, spectral density (for incommensurate case) obtained from the solution with "alternating" κ (dashed line in Fig.8(a)) is seen to be very close to that obtained from (12). This shows that "Ansatz" (12) and solution (14) produce results which are quantitatively close to an exact solution. Let us stress once again that our solution (14) is exact both for $\xi \to \infty$ and $\xi \to 0$, while in the region of finite ξ it provides rather good interpolation.

Consider now one-electron density of states:

$$N(E) = \sum_{\mathbf{p}} A(E, \mathbf{p}) = -\frac{1}{\pi} \sum_{\mathbf{p}} ImG^R(E\mathbf{p}) \tag{25}$$

which is determined by the integral of spectral density $A(E\mathbf{p})$ over the Brillouin zone. We have seen above that though for some topologies of the "bare" Fermi surface (band fillings) we can guarantee the same signs of velocity projections close to the "hot spots", this is not so in general case far from "hot spots", so that solution (14), based upon our "Ansatz" (12), is only approximate. Accordingly, the use of (14) to calculate the density of states with (25) leads also to a kind of approximation. In Fig.9 we show densities of states obtained from (13),(14),(25), with the use of the "bare" spectrum (8) for different diagram combinatorics (15),(16),(17), for the values of $t'/t = -0.4$ (Fig.9(a)) and $t'/t = -0.6$ (Fig.9(b)). We can see that for $t'/t = -0.4$ there appears some dip in the density of states (pseudogap). This dip is relatively weakly dependent on the value of correlation length ξ (see insert in Fig.9(b)). If the band filling is appropriate and the Fermi level μ is somewhere in this energy region there are also "hot spots" at the Fermi surface. For $t'/t = -0.6$ the region of existence of "hot spots" is rather wide, but the pseudogap in the density of states is practically unobservable. We can see only the obvious smearing of Van-Hove singularity which is present in the absence of fluctuations.

III. MODEL OF "SUPERCONDUCTING" FLUCTUATIONS.

4. Model description and solution for the Green's function.

Pseudogap phenomena can also be probably explained using the ideas of fluctuation Cooper pairing at temperatures higher than superconducting transition temperature T_c [1,5–7]. Let us consider the simplest possible model approach to this problem. In Fig.10(a)

we show the self-energy diagram of the first order in fluctuation propagator of Cooper pairs for $T > T_c$. Anticipating the possibility of both usual s-wave and d-wave pairing, characteristic of HTSC-systems, we introduce the pairing interaction of the simplest (separable) form:

$$V(\mathbf{p},\mathbf{p}') = -Ve(\phi)e(\phi') \tag{26}$$

where ϕ is polar angle determining the direction of electronic momentum $\mathbf{p}$ in the plane, while for $e(\phi)$ we assume model dependence [26,27]:

$$e(\phi) = \begin{cases} 1 & s\text{-wave pairing} \\ \sqrt{2}\cos(2\phi) & d\text{-wave pairing} \end{cases} \tag{27}$$

Interaction constant V is as usual assumed to be non zero in some energy layer around the Fermi surface. Then the self-energy corresponding to Fig.10(a) takes the form:

$$\Sigma(\varepsilon_n\mathbf{p}) = \sum_{m\mathbf{p}} V_{eff}(i\omega_m\mathbf{q})G(i\omega_m - i\varepsilon_n, -\mathbf{p}+\mathbf{q}) \tag{28}$$

where effective interaction with SC–fluctuations can be written as:

$$V_{eff}(i\omega_m\mathbf{q}) = -\frac{Ve^2(\phi)}{1 - VT\sum_{n\mathbf{p}} G_0(i\varepsilon_n\mathbf{p})G_0(i\omega_m - i\varepsilon_n, -\mathbf{p}+\mathbf{q})e^2(\phi)} \tag{29}$$

In the following we assume SC–fluctuations static [4]so that in (33) we can limit ourselves only to the term with $\omega_m = 0$. Then effective interaction can be written as:

$$V_{eff}(\mathbf{q}) \approx -\frac{\tilde{\Delta}^2 e^2(\phi)}{\xi^{-2}(T) + \mathbf{q}^2} \tag{30}$$

where

$$\xi(T) = \frac{\xi_0}{\sqrt{\frac{T-T_c}{T_c}}} \qquad ; \qquad \xi_0 \approx 0.18\frac{v_F}{T_c} \tag{31}$$

is the usual coherence length of superconductor, $\tilde{\Delta}^2 = \frac{1}{N(E_F)\xi_0^2}$ ($N(E_F)$–density of states at the Fermi level E_F). Surely, within the simplest BCS-like model used here, we have $\tilde{\Delta} \approx 2\pi^2 T_c(T_c/E_F) \sim \Delta_0(\Delta_0/E_F) \ll \Delta_0$ (where Δ_0 is superconducting energy gap at $T = 0$) and an obvious problem to explain the experimentally observable scale of pseudogap anomalies appears. However, in the following we again consider both ξ and $\tilde{\Delta}$ as some phenomenological parameters to be determined from experiment on HTSC-systems and not from naive BCS-like model.

---

[4]Static approximation here is valid for $\pi T \gg \omega_{sc} = 8(T - T_c)/\pi$, which is formally analogous to the condition of $\pi T \gg \omega_{sf}$ used in the "hot spot" model above. Here it is well satisfied if the system is close enough to superconducting transition

Analogously to transition from (2) to (4) we introduce instead of (30) the model interaction of the form:

$$V_{eff}(\mathbf{q}) = -\Delta^2 e^2(\phi)\frac{2\xi^{-1}}{\xi^{-2}+q_x^2}\frac{2\xi^{-1}}{\xi^{-2}+q_y^2} \tag{32}$$

where $\Delta^2 = \tilde{\Delta}^2/4$. Quantitatively this is close enough to (30) and leads to great simplification of calculation allowing us to classify contributions of higher order diagrams. In this case the first order contribution of diagram in Fig.10(a) is:

$$\Sigma^{(1)}(\varepsilon_n \mathbf{p}) = \frac{\Delta^2 e^2(\phi)}{i\varepsilon_n + \xi_{\mathbf{p}} + i(|v_x| + |v_y|)\kappa sign\varepsilon_n} \tag{33}$$

where $v_x = v_f \cos\phi$,$v_y = v_F \sin\phi$,$\kappa = \xi^{-1}$. Second order contribution from Fig.10(b) is:

$$\Sigma^{(2)}(\varepsilon_n \mathbf{p}) = (\Delta^2 e^2(\phi))^2 \int \frac{dq_{1x}}{\pi}\frac{\kappa}{\kappa^2+q_{1x}^2}\int \frac{dq_{1y}}{\pi}\frac{\kappa}{\kappa^2+q_{1y}^2}\int \frac{dq_{1x}}{\pi}\frac{\kappa}{\kappa^2+q_{2x}^2}\int \frac{dq_{1y}}{\pi}\frac{\kappa}{\kappa^2+q_{2y}^2}$$
$$\frac{1}{(i\varepsilon_n + \xi_{\mathbf{p}} - \mathbf{v_1 q_1})^2}\frac{1}{i\varepsilon_n - \xi_{\mathbf{p}} - \mathbf{v_2 q_1} - \mathbf{v_2 q_2}} \tag{34}$$

where $\mathbf{v}_1 = -\mathbf{v}_2 = \mathbf{v}_F$. In fact we can easily see that in this problem we have practically the same rules of diagram technique as in the "hot spot" model, but with combinatorics of incommensurate case. This last fact is obvious from the topology of interaction line (fluctuation propagator of Cooper pairs) in diagram of Fig.10(a) — it is seen that in higher orders only those diagrams exist in which interaction lines envelop only even number of interaction vertices. The expression of (34) is quite analogous to that of (9), but the signs of velocity projections in denominators of Green' functions here are always different: $\mathbf{v}_1 = -\mathbf{v}_2$. Thus in diagrams of higher orders there appear contributions not only from Lorentzians of interaction, but also from the Green's functions. However (in view of discussion in Appendix A) we can estimate contributions of higher order diagrams using the "Ansatz" of the type of (12), i.e. calculate all integrals e.g. in (34), as if velocity projections $\mathbf{v}_1$ and $\mathbf{v}_2$ are of the same sign, but in *answer* just put $\mathbf{v}_1 = -\mathbf{v}_2 = \mathbf{v}_F$. Then we again obtain the recurrence relation for the Green's function of the type of (14):

$$\Sigma_k(\varepsilon_n \xi_{\mathbf{p}}) = \frac{\Delta^2 e^2(\phi) v(k)}{i\varepsilon_n - (-1)^k \xi_{\mathbf{p}} + ikv_F\kappa(|\cos\phi| + |\sin\phi|) - \Sigma_{k+1}(\varepsilon_n \xi_{\mathbf{p}})} \tag{35}$$

where $v(k)$ is defined in (16). Surely, this relation (35) is not exact, but again it gives exact results for the limits of $\kappa \to 0(\xi \to \infty)$ and $\kappa \to \infty(\xi \to 0)$ and provides rather good (quantitatively) interpolation between these limits for the case of finite correlation lengths.

5. Spectral density and density of states.

In Fig.11(a) we show energy dependencies of the spectral density $A(E\mathbf{p})$ for one-particle Green's function (24), calculated from (35) for different values of polar angle ϕ, determining the direction of electronic momentum in the plane (we take here $|\mathbf{p}| = p_F$), for the case of fluctuations of d-wave pairing. It is clearly seen that in the vicinity of the point $(\pi/a, 0)$

in Brillouin zone this spectral density is non Fermi-liquid like (pseudogap). As vector $\mathbf{p}$ rotates in the direction of the zone diagonal the two peak structure gradually disappears and spectral density transforms to the typical Fermi-liquid like with a single peak, which is narrows as ϕ approaches $\pi/4$. Analogous transformation of the spectral density takes place as correlation length ξ becomes smaller.

In Fig.11(b) we also show the evolution of the product $f(E)A(E\mathbf{p})$ (where $f(E)$ is fermi distribution) which is essentially the parameter measured in ARPES experiments [2]. Note that curves in Fig.11(b) are quite similar to those obtained in Refs. [11,12] within the "hot spots" model. This picture of Fermi-surface destruction following from this calculations is qualitatively shown in Fig.12 and is very similar to experimental data obtained e.g. in Ref. [28] for $Bi_2Sr_2CaCu_2O_{8+\delta}$.

In case of fluctuation pairing of s-wave type the pseudogap appears isotropically on the whole Fermi-surface and spectral density is non Fermi-liquid everywhere for the case of large enough correlation lengths ξ of SC–fluctuations.

In Fig.13 we present the results of calculations of one-electron density of states with the help of (35) both for the case of s-wave pairing (Fig.13(a)) and d-wave pairing (Fig.13(b)), for different values of correlation length of SC–fluctuations. We see that in the case of d-wave pairing the pseudogap is the density of states is naturally not so deep as in s-wave case, even for large enough correlation lengths. At the same time it is seen that the pseudogap in the density of states in the model of SC–fluctuations is nevertheless much more expressive than in the model of "hot spots" due to AFM–fluctuations.

IV. CONCLUSION.

In this paper we have studied "nearly exactly" solvable models of the pseudogap state of the electronic spectrum of two-dimensional systems, based upon alternative scenarios of its origin — the picture of fluctuations of "dielectric" (AFM, SDW, CDW) type, leading to the model of of "hot spots", and the picture of fluctuational Cooper pairing above T_C (SC–fluctuations). The term "nearly exactly" solvable means that in this approach we can sum all Feynman diagram series for one-particle Green's function (and in fact also for two-particle Green' function [16,17]), using for the higher order diagrams an *approximate* "Ansatz" (12). As shown in Appendix A and also on numerical examples in the main part of the paper this "Ansatz" guarantees rather good (quantitatively) approximation to an exact solution in the region of finite correlation lengths of fluctuations of short range order ξ, while in the limits of $\xi \to \infty$ and $\xi \to 0$ our solution is exact.

Calculation of the spectral densities shows that within both scenarios we can obtain rather attractive (in the sense of possible comparison with the experimental data on cuprates) picture of "destruction" of Fermi-liquid behavior on specific ("hot") parts of the Fermi-surface, with persistence of Fermi-liquid state on the rest ("cold") part of the Fermi-surface. This non Fermi-liquid behavior is due to the strong scattering of electrons on fluctuations of short range order and, in general, is more visible with the growth of correlation length ξ. At the same time there are definite differences between these two scenarios which can be used, in principle, in the analysis of real experimental situation. In particular, in the "hot spots" model (AFM–fluctuations) the pseudogap in the density of states is relatively weak (cf. Fig.9), while in the model of SC–fluctuations the pseudogap in the

density of states is more visible (cf. Fig.13). The model of "dielectric" AFM–fluctuations is more attractive even from simplest consideration of the phase diagram of Fig.1 — pseudogap anomalies are mainly observed in the underdoped region and are apparently more intensive for systems which are closer to dielectric (AFM) state. It is obvious that precisely in this region we can expect more important role of fluctuations of "dielectric" (AFM) type and the growth of corresponding correlation length ξ. It is rather difficult to imagine why in this region of the phase diagram SC–fluctuations may become more important, this apparently must take place somewhere close to the optimal (corresponding to highest T_c) doping. Also in SC–scenario we have an obvious problem of characteristic scales (on temperature and energy) of pseudogap anomalies, which can not be solved within simple BCS-like theory, and requires some new microscopic approaches [5,7]. Our models are useful for the analysis within both scenarios of pseudogap formation irrespective of microscopic picture, because they are based on rather general (semi phenomenological) form of correlation function of fluctuations of short range order.

Authors are grateful to O.V.Tchernyshyov for preliminary information on his analysis of one-dimensional model.

This work is partly supported by Russian Basic Research Foundation under the grant No.96-02-16065, as well as by projects No.IX.1 of the State Program "Statistical Physics" and No.96-051 of the State Program on HTSC of the Russian Ministry of Science.

APPENDIX A: ANALYSIS OF ONE-DIMENSIONAL MODEL.

Let us consider in more detail the use of the "Ansatz" (12) to estimate the contributions of higher order diagrams. We shall limit ourselves to the analysis of one-dimensional model [15–17], because in one-dimension the problem is most serious [22]. We are interested in the vicinity of Fermi "points" $+p_F$ $-p_F$, while the Gaussian fluctuations of short range order scatter electrons by the momentum of the order of $Q \sim^{+}_{-} 2p_F$ from one end of the Fermi "line" to the opposite with scattering momentum values fixed with precision of the order of $\xi^{-1} = \kappa$ [13–17]. We shall consider the linearized electronic spectrum: $\xi_{p^{-}_{+}p_F} =^{+}_{-} v_F p$ and to shorten notations put $v_F = 1$. Thus our system consists of "two types" of electrons — those moving to the "left" and to the "right". It is convenient to make our analysis in the coordinate representation [22], when the equation of motion of electrons in our model takes the form [18,22]:

$$\Big(i\hat{1}\frac{\partial}{\partial t} - i\hat{\sigma}_3\frac{\partial}{\partial x}\Big)\hat{\Psi}(t,x) = \begin{pmatrix} 0 & \Delta(x) \\ \Delta^{\star}(x) & 0 \end{pmatrix}\hat{\Psi}(t,x) \tag{A1}$$

We limit ourselves with incommensurate fluctuations only when $\Delta^{\star}(x) \neq \Delta(x)$. Spinor $\hat{\Psi} = \begin{pmatrix} \psi_{+} \\ \psi_{-} \end{pmatrix}$ describes "right" and "left" electrons. Fluctuations $\Delta(x)$ are supposed to be Gaussian with $< \Delta(x) = 0 >$ and $< \Delta^{\star}(x)\Delta(x') >= |\Delta|^2 exp(-\kappa|x - x'|)$. Free propagator in frequency and coordinate representation has the form:

$$G_0(\varepsilon x) = i\theta(\varepsilon\sigma_3 x)sign(\varepsilon)exp(i\varepsilon\sigma_3 x) \tag{A2}$$

where $\sigma_3 = +1$ for the "right" particles, $\sigma_3 = -1$ for the "left". The particle passing the path of the length l produces a phase factor $e^{i\varepsilon l}$. During calculation of contribution of a given diagram it is convenient to change integration variables from coordinates of interaction vertices x_k to path lengths l_k, passed by the particle between scattering events [22]. It is important to take into account the fact that these path lengths are not independent as for the given diagram the total particle displacement $x - x'$ is fixed. The rules of the diagram technique to calculate $G(\varepsilon, x - x')$ are as follows [22]:

1. Electron line of length l_k gives the factor $-ie^{il_k(\varepsilon - (-1)^k p)}$.
2. Wavy (interaction) line connecting vertices m and n gives the factor:
   $|\Delta|^2 exp(-\kappa|x_m - x_n|) = |\Delta|^2 exp(-\kappa|\sum_{k=m}^{n-1}(-1)^k l_k|)$.
3. Over all l_k we must integrate from 0 to ∞.
4. Integrate over p with a factor of $e^{ip(x-x')}/2\pi$.

To calculate $G(\varepsilon p)$ just drop the last rule. From these rules we can see that the finite values of correlation length $\xi = \kappa^{-1}$ lead to some damping of given transition amplitude with the displacement of the particle. The exact accounting of this effect is rather complicated but we can find some upper and lower bound estimates. Considering first the obvious inequality:

$$exp\Big(-\kappa|\sum_{k=m}^{n-1}(-1)^k l_k|\Big) > exp\Big(-\kappa\sum_{k=m}^{n-1} l_k\Big) \tag{A3}$$

and using for the interaction line the r.h.s. expression in (A3), we overestimate transition amplitude damping (i.e. effectively overestimate κ) for the given diagram. It is easy to see that the use of this approximation to calculate a given diagram for the Green's function leads (in momentum representation) to an extra $\imath\kappa$ appearing in every denominator of Green's function enveloped by an extra interaction line. This leads to an expression for the given higher order contribution of the form of (12) (cf. [22]). For example, diagram shown in Fig.14 yields (we assume $\varepsilon > 0$, $\delta = 0^+$):

$$\Delta G(\varepsilon p) = \Delta^4 \frac{1}{\varepsilon - p + i\delta}\Big(\frac{1}{\varepsilon + p + i\kappa}\frac{1}{\varepsilon - p + 2i\kappa}\frac{1}{\varepsilon + p + i\kappa}\Big)\frac{1}{\varepsilon - p + i\delta} \tag{A4}$$

which is analogous to (9),(11). On the other hand we can take the inequality:

$$exp\Big(-\kappa|\sum_{k=m}^{n-1}(-1)^k l_k|\Big) < exp\Big(-\kappa\sum_{k=m}^{n-1}(-1)^{k-m} l_k\Big) \tag{A5}$$

and use for the interaction line the r.h.s. expression in (A5). This will lead to some underestimation of damping effect in the given transition amplitude (i.e. effectively underestimate κ). [5] In particular, for diagram in Fig.14 the contribution of interaction lines is:

$$e^{-\kappa l_2} e^{-\kappa|l_1 - l_2 - l_3|} \to e^{-\kappa l_2} e^{-\kappa(l_1 - l_2 + l_3)} = e^{-\kappa(l_1 + l_3)} \tag{A6}$$

In momentum representation this yields:

$$\Delta G(\varepsilon p) = \Delta^4 \frac{1}{\varepsilon - p + i\delta}\Big(\frac{1}{\varepsilon + p + i\kappa}\frac{1}{\varepsilon - p + i\delta}\frac{1}{\varepsilon + p + i\kappa}\Big)\frac{1}{\varepsilon - p + i\delta} \tag{A7}$$

Analysis of higher order diagrams shows that in this case contributions of all diagrams of the N-th order are equal and in the momentum representation we have ("Ansatz of alternating κ"):

$$G_N(\varepsilon p) = |\Delta|^{2N} \frac{1}{(\varepsilon - p + i\delta)^{N+1}}\frac{1}{(\varepsilon + p + i\kappa)^N} \tag{A8}$$

Then the whole series is easily summed analogously to the case of $\kappa = 0$ [13,14] and we obtain the Green's function in the form:

---

[5] It may seem that this choice for the interaction line contribution can even lead to the growth of transition amplitude in comparison with the case of $\kappa = 0$ and to appearance of some divergences, but this is not so. As we consider only incommensurate case here, where the interaction line envelopes only even number of interaction vertices (i.e. an odd number of l_k), the choice of the sign in the exponent after removing the modulous is determined by dominance of even or odd l_k. This leads to effective damping of any diagram in higher orders.

$$G^R(\varepsilon p) = \sum_{N=0}^{\infty} N! G_N(\varepsilon p) = \int_0^{\infty} d\zeta e^{-\zeta} \frac{\varepsilon + p + i\kappa}{(\varepsilon - p + i\delta)(\varepsilon + p + i\kappa) - \zeta|\Delta|^2} \tag{A9}$$

From this expression we can easily calculate the spectral density or the density of states:

$$\frac{N(\varepsilon)}{N(E_F)} = \frac{v_F \kappa}{\pi} \int_{-\infty}^{\infty} d\xi_p \int_0^{\infty} d\zeta e^{-\zeta} \frac{\zeta|\Delta|^2}{(\varepsilon^2 - \xi_p^2 - \zeta|\Delta|^2)^2 + (v_F\kappa)^2(\varepsilon - \xi_p)^2} \tag{A10}$$

where we have restored v_F explicitly. In Fig.15 we compare densities of states for different values of κ (correlation length), calculated using the "Ansatz of alternating κ" and recurrence relations similar to (12) in one-dimensional model [15–17]. We see that the results are quantitatively close practically for all values of κ. As we noted above our main "Ansatz"(12),(A4) somehow overestimates the role of finite κ, while the "Ansatz of alternating κ" (A7) underestimates it. Then it is guessed that the exact value of the density of states is in fact quite close to those obtained using these two types of approximation for the higher order diagrams. Analogous results can be obtained also for spectral densities. In fact this means that the results for the main physical quantities determined by one-electron Green's functions are not strongly dependent on the way the finite κ enter the expressions for diagrams of higher order, but the main thing is to take account (at least approximately) of *all* diagrams of perturbation theory with different combinatorics. In principle this is not very surprising, as the main effect of pseudogap formation is due essentially to "backward" $Q \sim 2p_F$–scattering, which is accounted for exactly in the limit of $\xi \to \infty$, while the effect of finite κ reduces to rather weak modulation of this random field, leading to the damping of its correlator and smearing of the pseudogap.

Naturally, the "Ansatz of alternating κ" can be written in the form of recurrence relation of the type of (14) also for two-dimensional, models discussed in the main part of this paper. For example in "hot spots" model we have:

$$\Sigma_k(\varepsilon_n \xi_{\mathbf{p}}) = \Delta^2 \frac{v(k)}{i\varepsilon_n - \xi_k + i\alpha_k v_k \kappa - \Sigma_{k+1}(\varepsilon_n \xi_{\mathbf{p}})} \tag{A11}$$

where $\alpha_k = 1$ for odd k and $\alpha_k = 0$ for even k. Other notations are given above in the main part. Data for the density of states obtained with the help of (A11) are shown above in Fig.9 and confirm the our conclusions. Expression similar to (A11) can be easily written also for the model of SC–fluctuations.

Let us stress that the "Ansatz of alternating κ" is rather formal and is used only to show that this more or less arbitrary "approximation", underestimating the role of finite κ in diagrams of higher orders, leads to results which are quantitatively close those obtained with the "Ansatz" (12),(A4), which overestimates this role. This last approximation used in Refs. [15–18] and in the main part of this article has much deeper sense. As we have already stated above this approximation is exact in the vicinity of "hot spots" for the values of parameters of the "bare" spectrum t,t' and μ (topologies of the Fermi surface) which guarantee equal signs of velocity projections in "hot spots" connected by vector $\mathbf{Q}$. Analogously in one-dimensional model it is possible to obtain the higher order contributions in the form similar to (12) or (A4) if we consider the model of correlator of fluctuations of short range order with the maximum at some arbitrary scattering vector Q which is much smaller than p_F, so that (for large enough correlation lengths ξ) electrons are scattered by

fluctuations remaining always on one ("left" or "right") branch of the spectrum. In this case expressions of the type of (A4) are exact. After that in final *answers* for diagrams of higher orders we can perform *continuation* to $Q \sim 2p_F$ of interest to us, as the only dependence on Q enters only via the "bare" electronic spectrum. Similarly we can achieve the same result changing appropriately the chemical potential μ (band filling).

REFERENCES

[1] M.Randeria. Varenna Lectures 1997, Preprint cond-mat/9710223
[2] M.Randeria, J.C.Campuzano, Varenna Lectures 1997, Preprint cond-mat/9709107
[3] H.Ding et al. Nature **382**,51(1996)
[4] H.Ding et al. Phys.Rev.Lett. **78**,2628(1997)
[5] V.B.Geshkenbein,L.B.Ioffe,A.I.Larkin. Phys.Rev. **B55**,3173(1997)
[6] V.Emery, S.A.Kivelson, O.Zachar. Phys.Rev. **B56**,6120(1997)
[7] J.Maly, B.Janko, K.Levin. Preprint cond-mat/9710187, 9805018
[8] A.P.Kampf,J.R.Schrieffer. Phys.Rev. **B41**,6399(1990), **B42**,7967(1990)
[9] V.Barzykin,D.Pines. Phys.Rev. **B52**,13585(1995)
[10] D.Pines. Tr.J. of Physics **20**,535(1996)
[11] J.Schmalian, D.Pines, B.Stojkovic. Phys.Rev.Lett. **80**, 3839(1998)
[12] J.Schmalian, D.Pines, B.Stojkovic. Preprint cond-mat/9804129.
[13] M.V.Sadovskii. Zh.Eksp.Teor.Fiz.**66**,1720(1974); Sov.Phys.-JETP **39**, 845 (1974)
[14] M.V.Sadovskii. Fiz.Tverd.Tela **16**,2504(1974); Sov.Phys.-Solid State **16**, 1632 (1974)
[15] M.V.Sadovskii. Zh.Eksp.Teor.Fiz.**77**, 2070(1979); Sov.Phys.-JETP **50**, 989 (1979)
[16] M.V.Sadovskii, A.A.Timofeev. Sverkhprovodimost' **4**, 11(1991)
[17] M.V.Sadovskii, A.A. Timofeev. J.Moscow Phys.Soc. **1**, 391(1991)
[18] R.H.McKenzie, D.Scarratt. Phys.Rev. **54**, R12709 (1996)
[19] O.Tchernyshyov. Phys.Rev. **B56**, 3372 (1997)
[20] H.C.Ren. Preprint cond-mat/9612184
[21] A.I.Posazhennikova, M.V.Sadovskii. Preprint cond-mat/9806199
[22] O.Tchernyshyov. Preprint cond-mat/9804318
[23] P.Monthoux, A.Balatsky, D.Pines. Phys.Rev. **B46**, 14803 (1992)
[24] P.Monthoux, D.Pines. Phys.Rev. **B47**, 6069 (1993), Phys.Rev. **B48**, 4261 (1994)
[25] P.V.Elyutin. Opt.Spectrosk.**43**, 542 (1977); Opt.Spectrosc.(USSR) bf 43, 318 (1977)
[26] L.S.Borkovski, P.J.Hirschfeld. Phys.Rev. **B49**, 15404 (1994)
[27] R.Fehrenbacher, M.R.Norman. Phys.Rev. **B50**, 3495 (1994)
[28] M.R.Norman et al. Preprint cond-mat/9710163

Figure Captions.

Fig.1. Schematic phase diagram of HTSC-cuprates [12]. For temperatures $T < T^{cr}$ there are well developed fluctuations of AFM short range order. For $T_* < T < T^{cr}$ these fluctuations can be considered as static.

Fig.2. Model of the Fermi surface for HTSC-cuprates. Electronic states around the intersection points of the Fermi surface with magnetic Brillouin zone (shown by dashed lines) are strongly interacting with fluctuations of AFM short range order ("hot spots").

Fig.3. First order self-energy diagram for the electron interacting with fluctuations of short-range order.

Fig.4. Second order sel-energy diagrams for the electron interacting with fluctuations of short range order.

Fig.5. Regions in spectrum parameters space where both "hot spots" exist (dashed region) and velocity projections in "hot spots " are of the same sign (doubly dashed region).

Fig.6. Fermi surfaces defined by the spectrum (8), for different values of the chemical potential μ (band-filling) and parameter t'/t.

(a)—case of $t'/t = -0.6$, when (14) is exact close to "hot spots":
$\mu/t =$: (1)— -2.2; (2)— -1.8; (3)— -1.666...; (4)— -1.63; (5)— -1.6; (6)— 0; (7)— 2,
solution (14) is exact in the vicinity of "hot spots"(velocity projections are of the same sign) for $\mu/t < -1.666\ldots$, "hot spots" exist for $\mu/t < 0$.

(b)—case of $t'/t = -0.4$, characteristic of HTSC-cuprates, when (14) is approximate:
$\mu/t =$: (1)— -2.2; (2)— -2; (3)— -1.6; (4)— -1.3; (5)— 0; (6)— 2; (7)— 4,
"hot spots" exist for $-1.6 < \mu/t < 0$.

Fig.7. Energy dependencies of the spectral density in the "hot spot" ($p_x a/\pi = 0.1666, p_y a/\pi = 0.8333$) for different diagram combinatorics for the case of $t'/t = -0.6$, when (14) is exact:

(a)—incommensurate case.

(b)—commensurate case.

(c)—combinatorics of spin-fermion model.

Correlation length corresponds to the values of κ: (1)—0.01; (2)—0.1; (3)—0.5,
$\Delta = 0.1t$.

At the inserts—energy dependencies of spectral density for different diagram combinatorics for $\kappa a = 0.01$

(1)—at the "hot spot" $p_x a/\pi = 0.1666$, $p_y a/\pi = 0.8333$.

(2)—close to the "hot spot" $p_x a/\pi = 0.1663$, $p_y a/\pi = 0.8155$.

(3)—far from the "hot spot" $p_x a/\pi = 0.0$, $p_y a/\pi = 0.333$.

Fig.8. Energy dependencies of the spectral density far from the "hot spot" ($p_x a/\pi = 0.142$, $p_y a/\pi = 0.857$) for $t'/t = -0.4$, $\mu/t = -1.3$, which is approximately valid for HTSC–cuprates:

(a)—incommensurate case. Dashed line—spectral density for incommensurate case obtained from (A11).

(b)—commensurate case.

(c)—combinatorics of spin-fermion model.

Correlation length corresponds to the values of κa: (1)—0.01; (2)—0.1; (3)—0.5, $\Delta = 0.1t$.

At the inserts — energy dependencies of spectral density for different diagram combinatorics for $\kappa a = 0.01$

(1)—at the "hot spot" $p_x a/\pi = 0.142$, $p_y a/\pi = 0.857$.

(2)—close to the "hot spot" $p_x a/\pi = 0.145$, $p_y a/\pi = 0.843$.

(3)—far from the "hot spot" $p_x a/\pi = p_y a/\pi = 0.375$.

Fig.9. One-electron density of states for different diagram combinatorics ((a)–case of $t'/t = -0.4$, $\mu/t = -1.3$; (b)–case of $t'/t = -0.6$,$\mu/t = -1.8$):

(1)—incommensurate case.

(2)—commensurate case.

(3)—combinatorics of spin-fermion model.

(4)—in the absence of AFM fluctuations.

Dashed line—incommensurate case, obtained from (A11).

$\Delta/t = 1$, correlation length corresponds to $\kappa a = 0.1$.

At the inserts—one-electron density of states for commensurate combinatorics for:

(1)—$\kappa a = 0.1$; (2)—$\kappa a = 0.01$

Fig.10. Self-energy diagrams in the model of SC–fluctuations:

(a)—first order diagram with explanation of the meaning of interaction line (fluctuation propagator of Cooper pairs).

(b)—second order diagram.

Fig.11. (a)–Energy dependence of the spectral density $A(E, \mathbf{p})$ for the case of d-wave fluctuation pairing for different values of the polar angle ϕ, defining the direction of electronic momentum in the plane:

(1)—$\phi = 0$; (2)—$\phi = \pi/6$.

Correlation length corresponds to $v_F\kappa/\Delta = 0.5$ (full curve) and 0.1 (dashed).

(b)–analogous dependence of the product $f(E)A(E, \mathbf{p})$ ($f(E)$– Fermi function):

(1)—$\phi = 0$; (2)—$\phi = \pi/6$; (3)—$\phi = \pi/4.83$.

Temperature (in Fermi function) $T = 0.1\Delta$, $v_F\kappa/\Delta = 0.5$.

Fig.12. Schematic picture of Fermi surface "destruction" by pseudogap due to fluctuational d-wave pairing. Dashed are the regions, where the spectral density is essentially non Fermi-liquid like.

Fig.13. One-electron density of states in the model of SC–fluctuations for the different values of parameter $v_F\kappa/\Delta$:

(a)—case of s-wave pairing.

(b)—case of d-wave pairing.

Curves are shown for the following values of $v_F\kappa/\Delta$:

(1)—0.1; (2)—0.5; (3)—1.0; (4)—2.0.

Fig.14. Second order diagram for the correction to the Green's function in coordinate representation.

Fig.15. One-electron density of states in one-dimensional model for the different values of $v_F\kappa/\Delta$:

(1)—0.1; (2)—0.8; (3)—1.2.

Full curves — result of calculations using (12),(14) [15], dashed line — result of calculations using (A10).

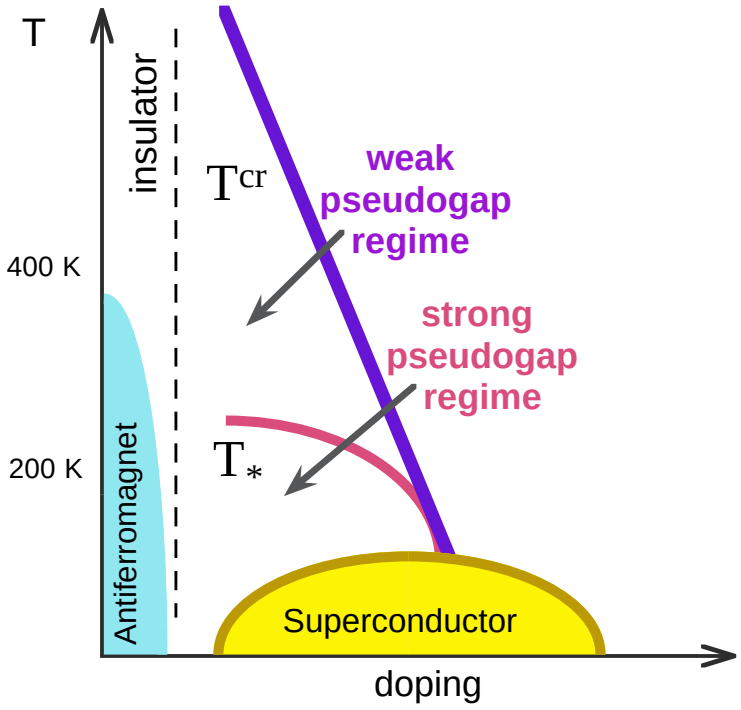

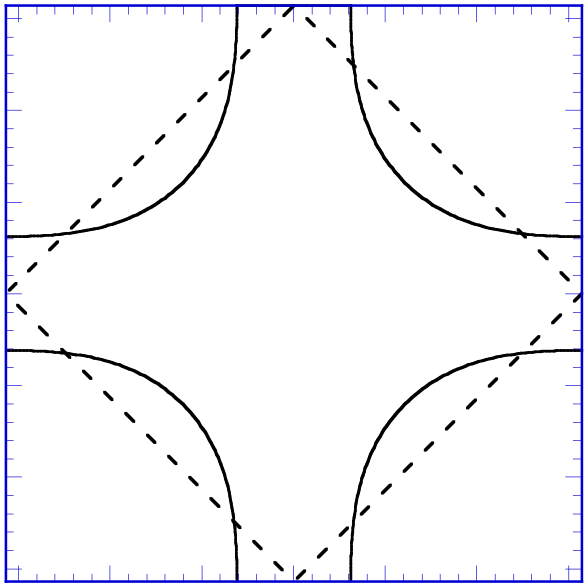

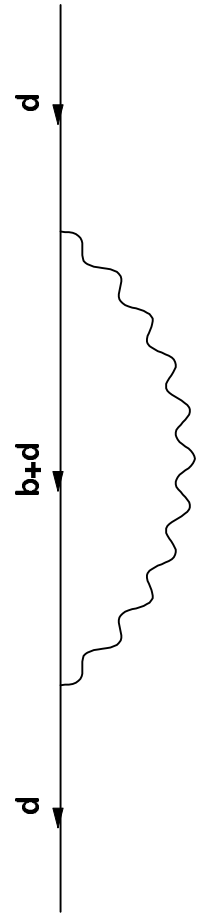

Fig.3

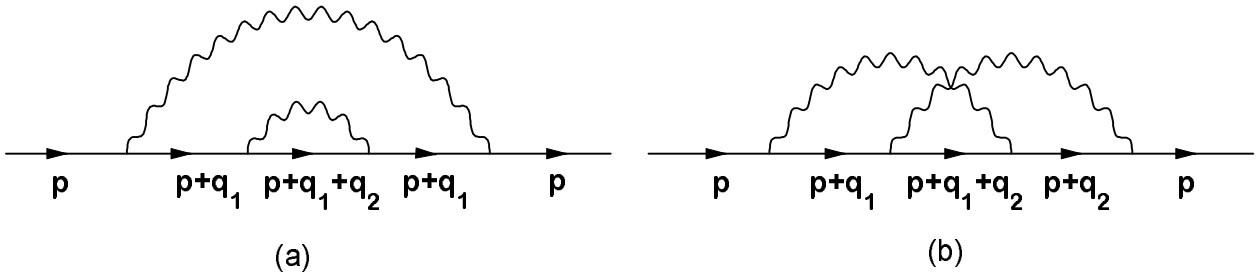

Fig.4

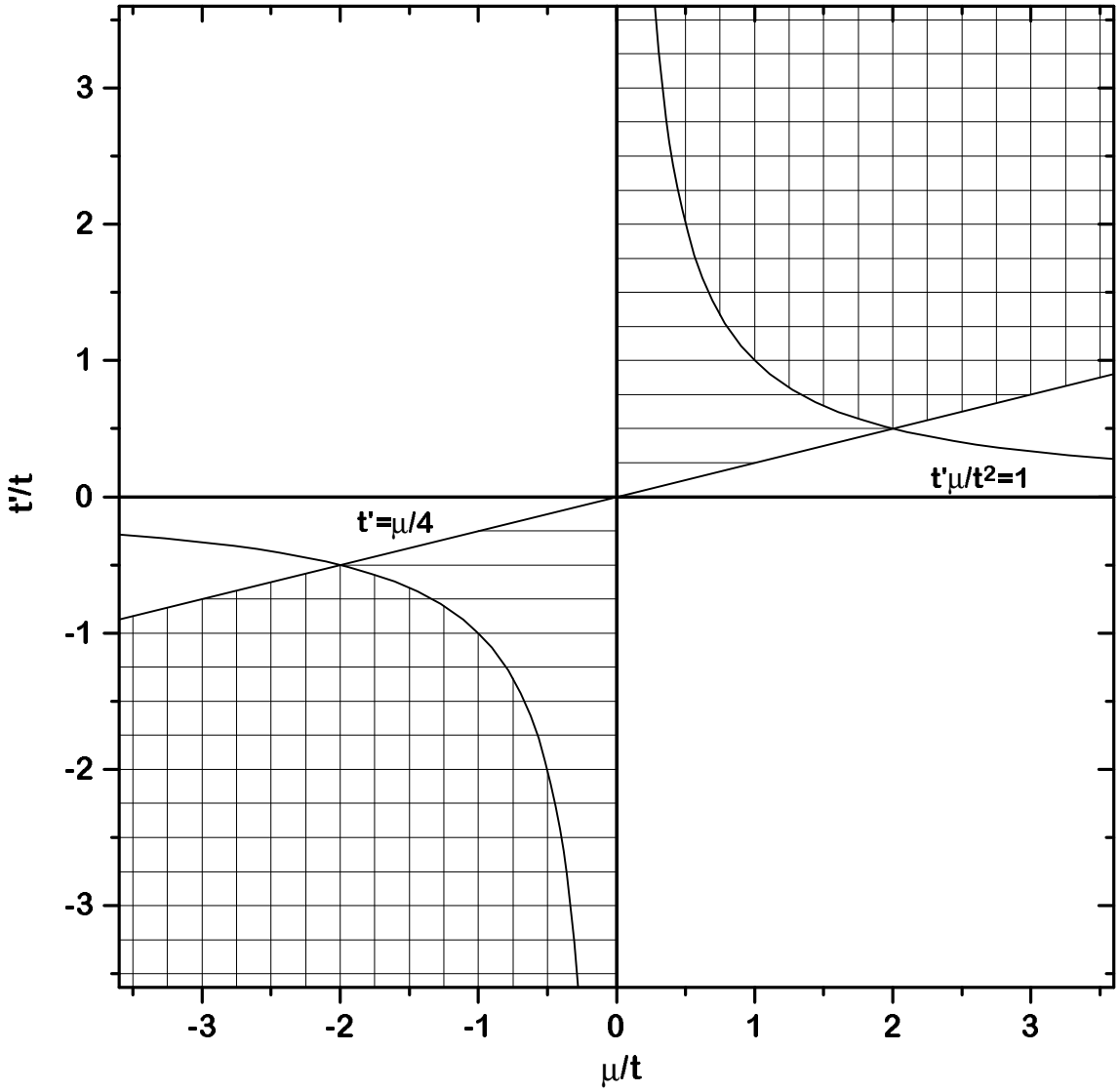

Fig.5

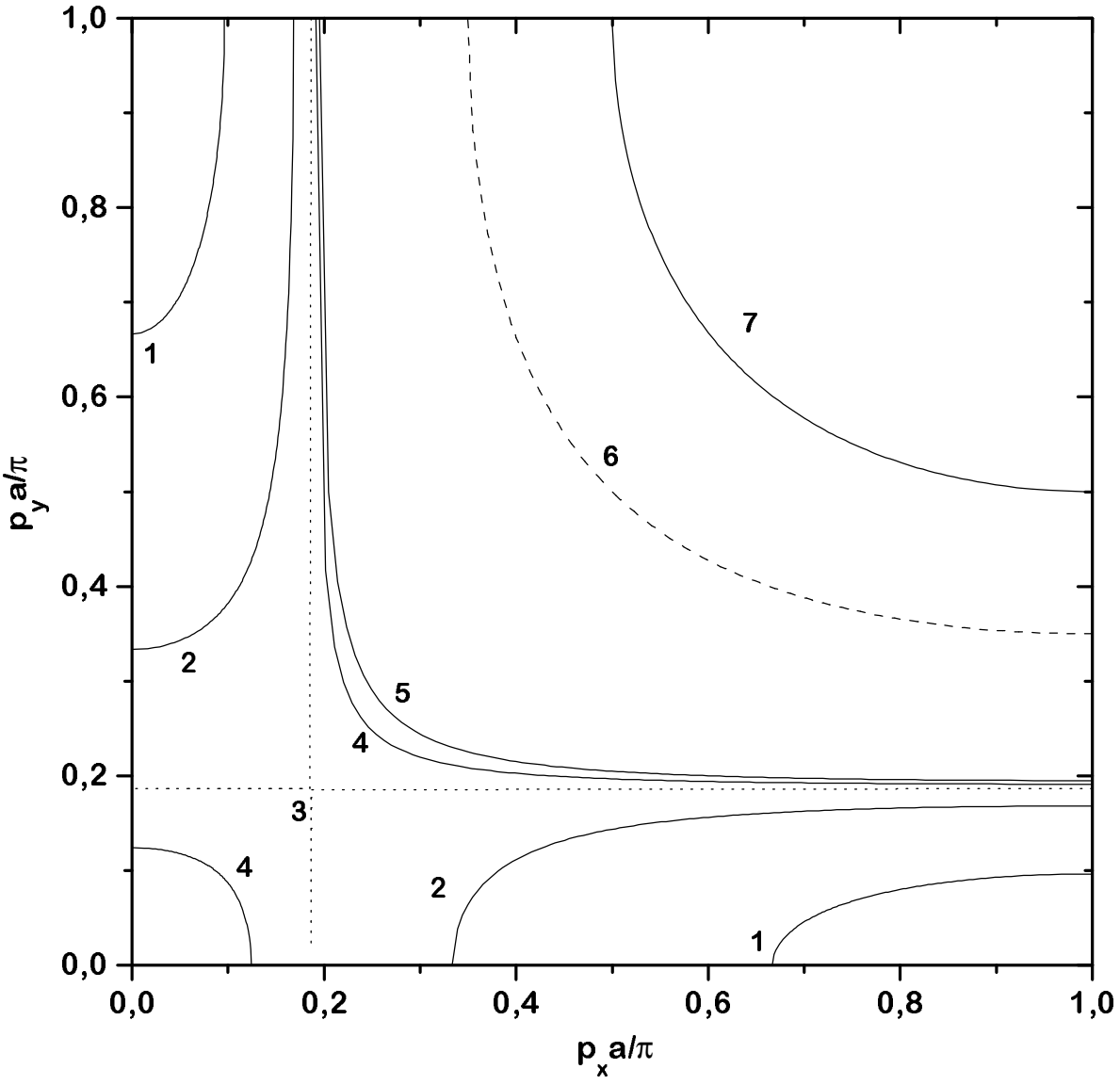

Fig.6(a)

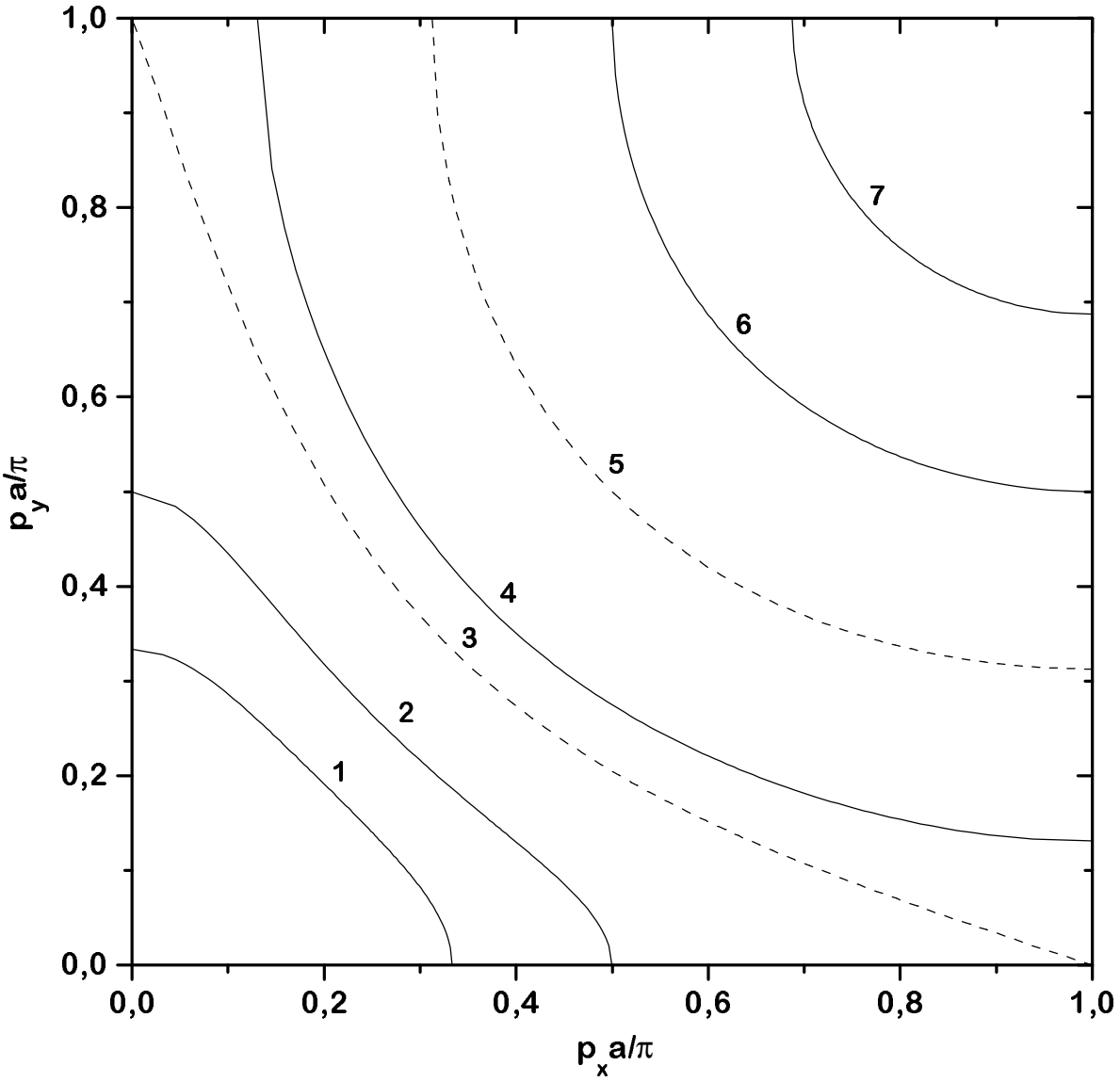

Fig.6(b)

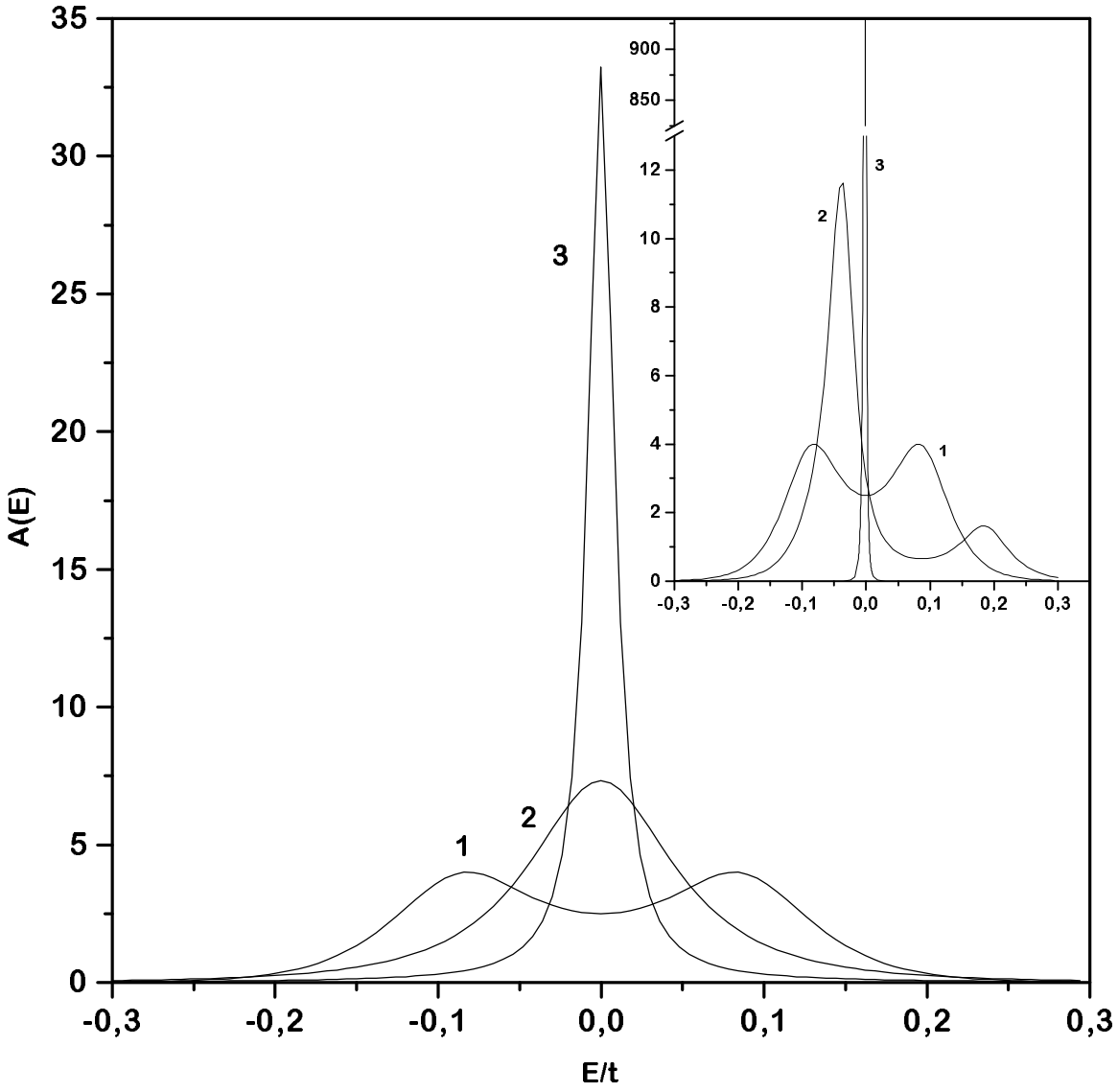

Fig.7(a)

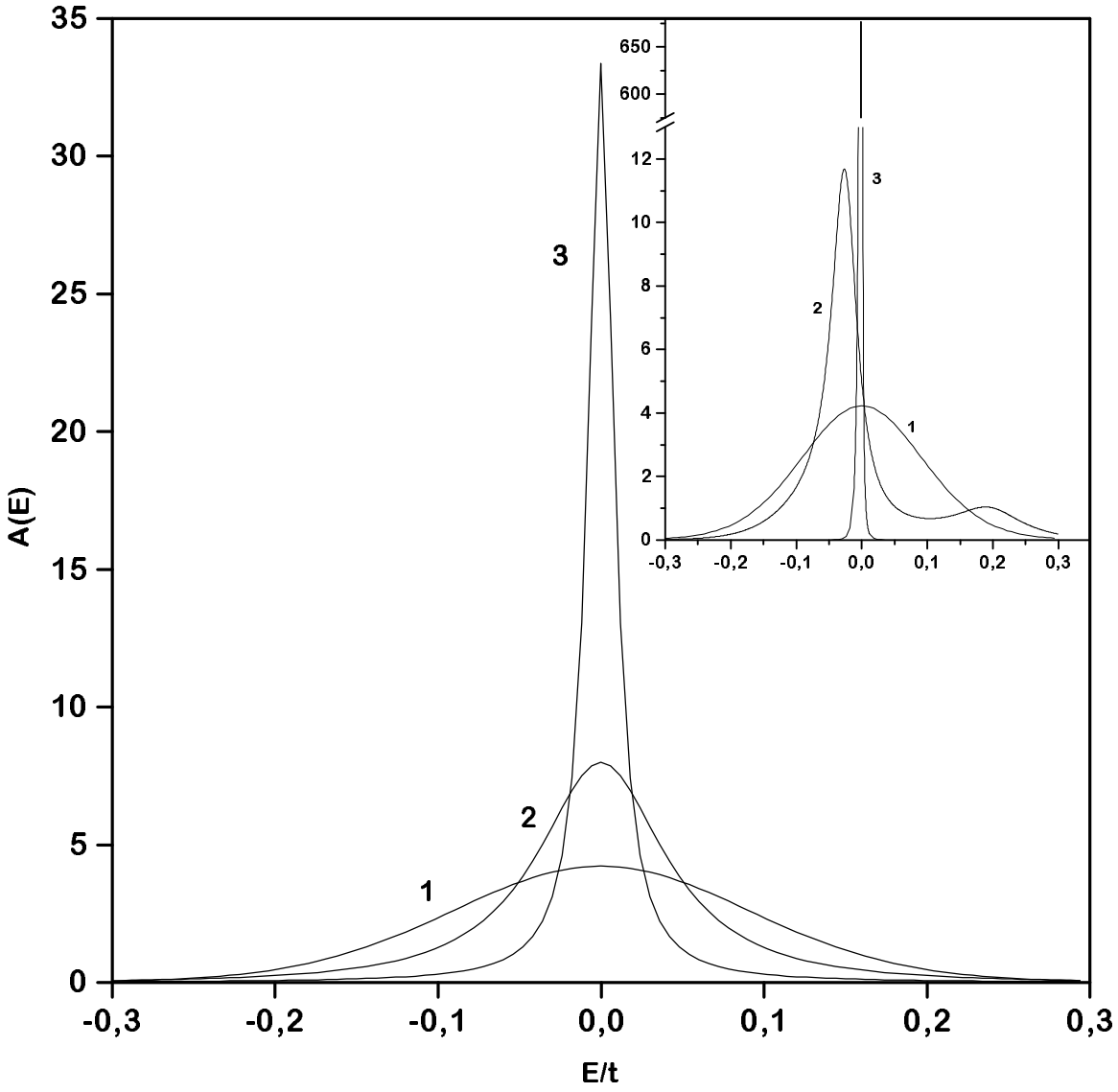

Fig.7(b)

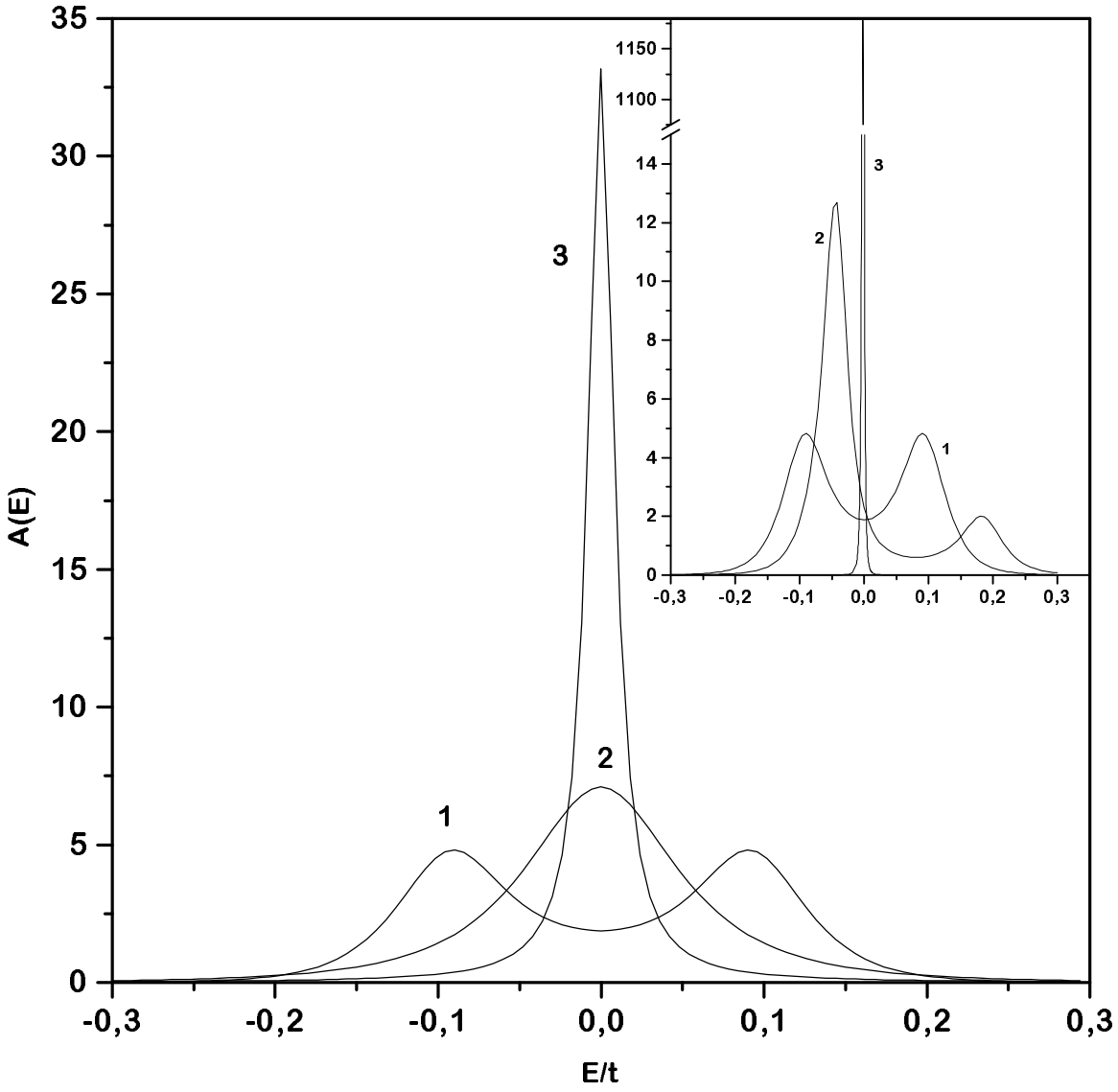

Fig.7(c)

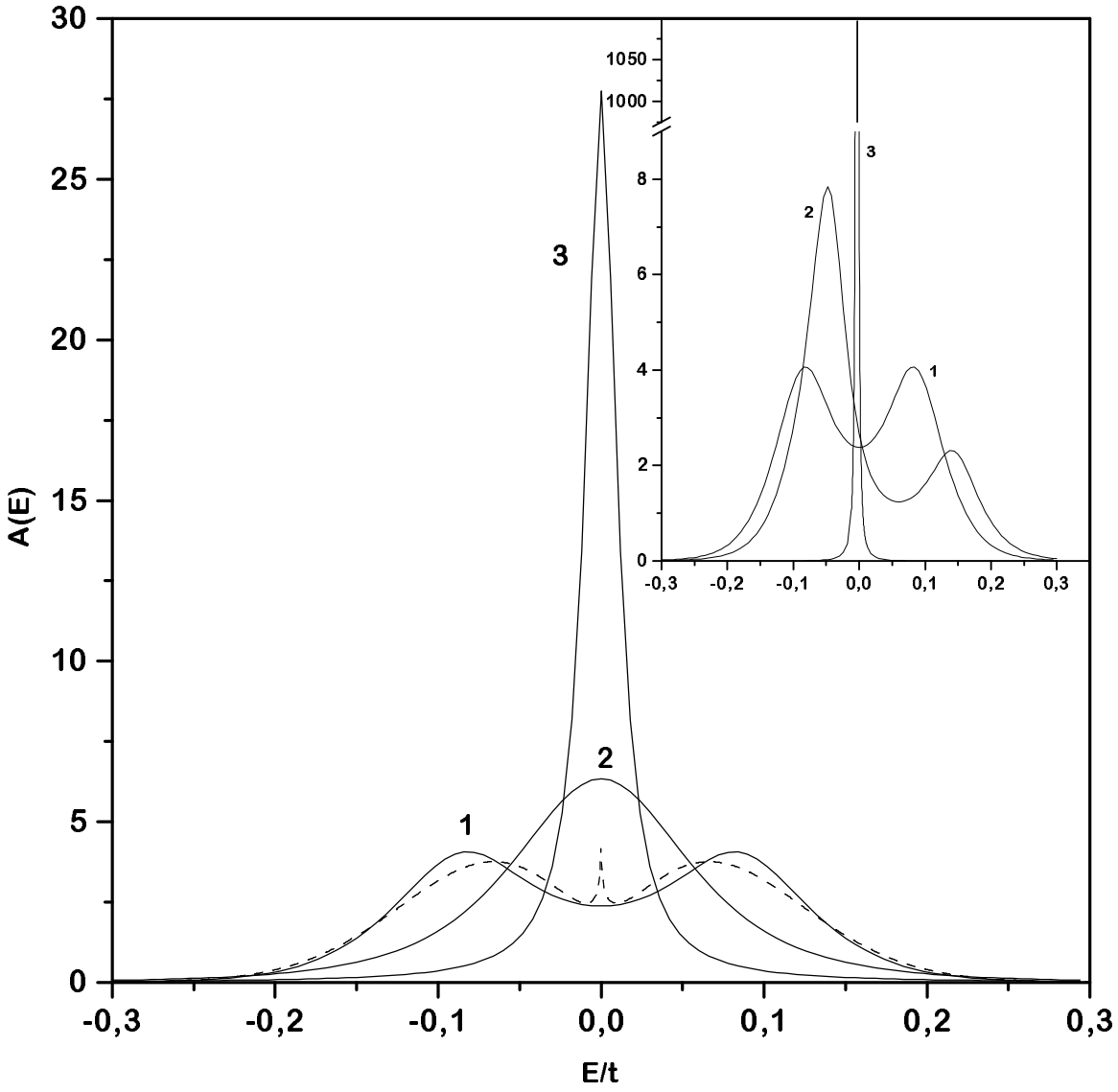

Fig.8(a)

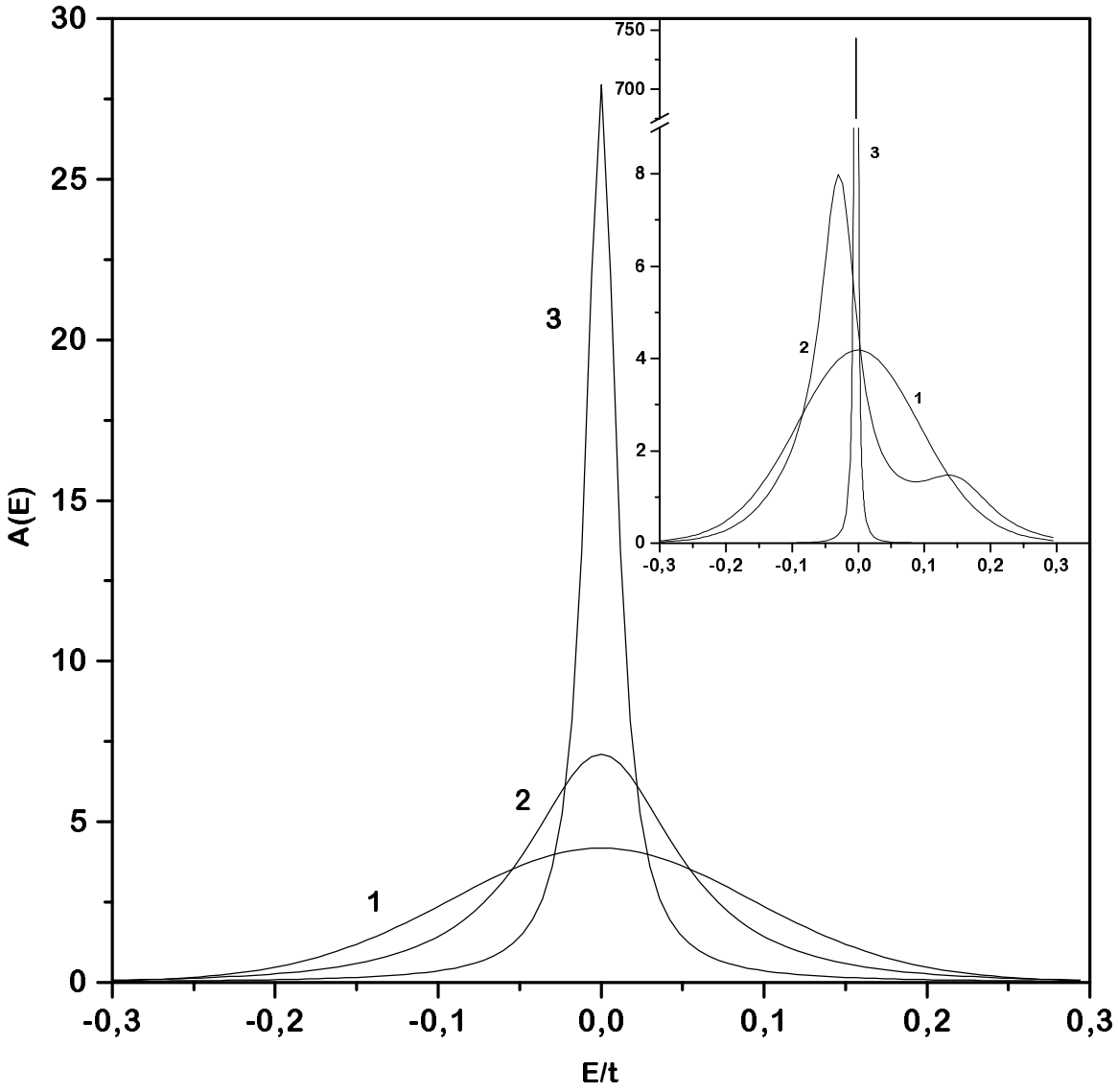

Fig.8(b)

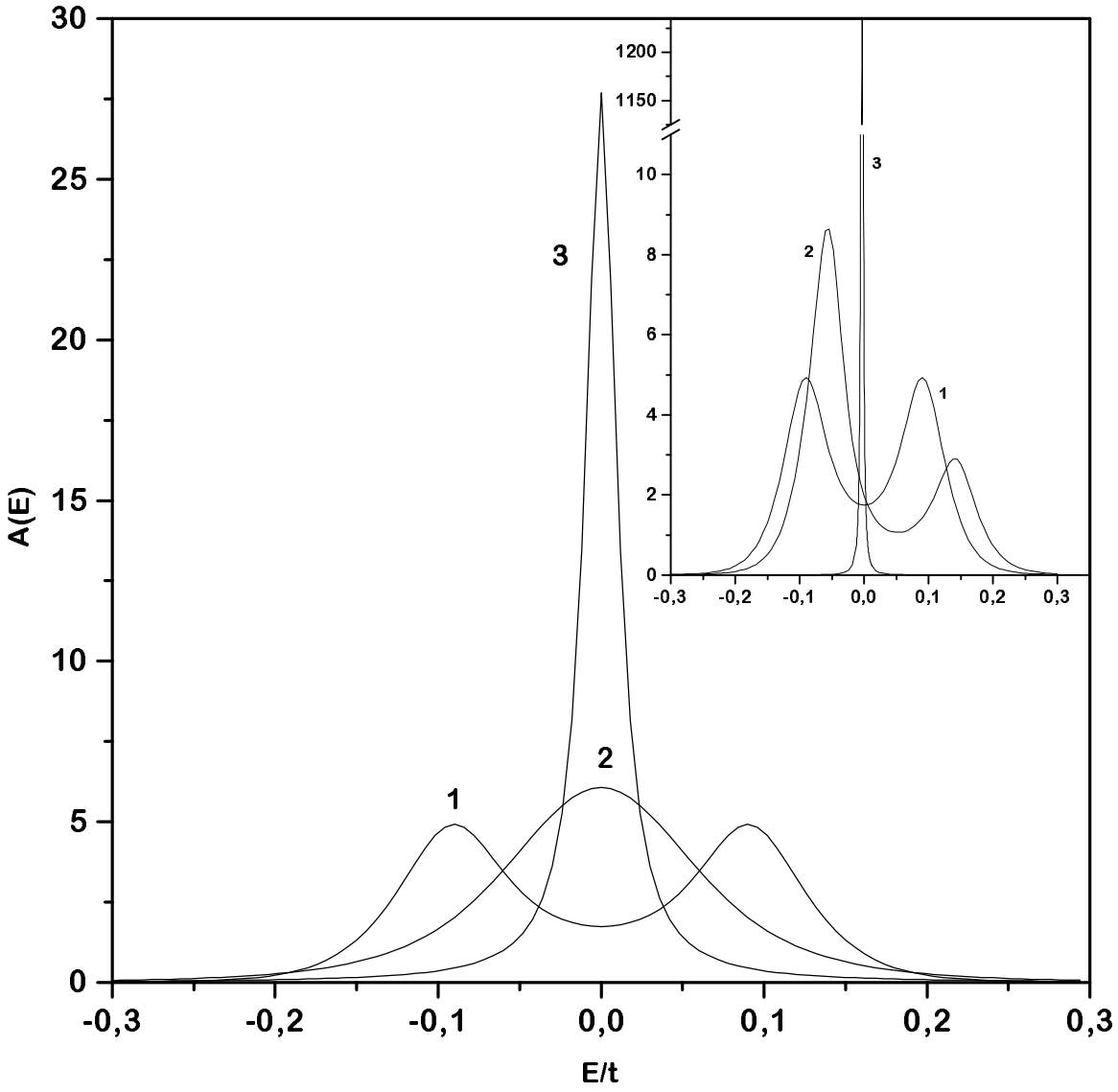

Fig.8(c)

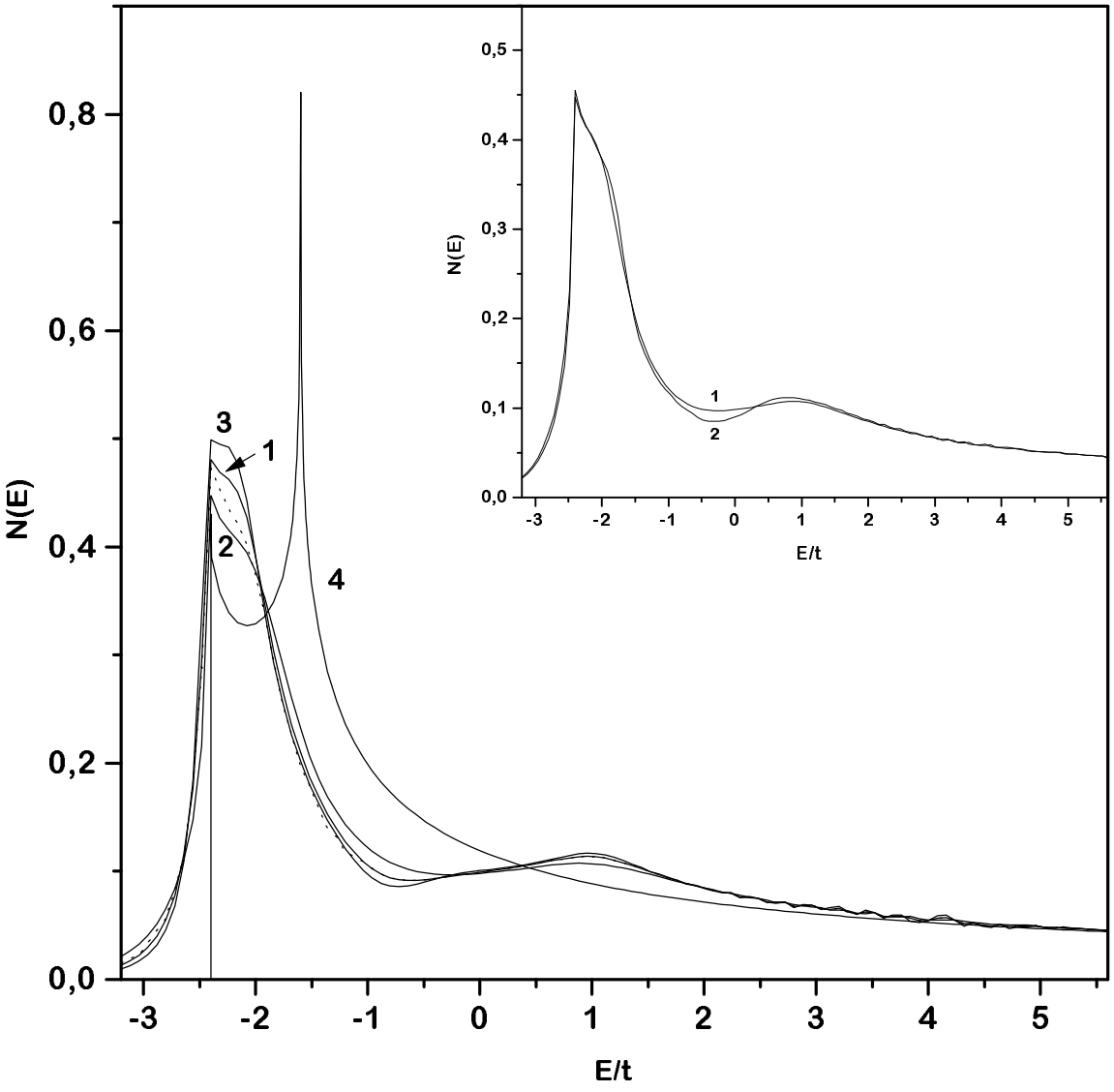

Fig.9(a)

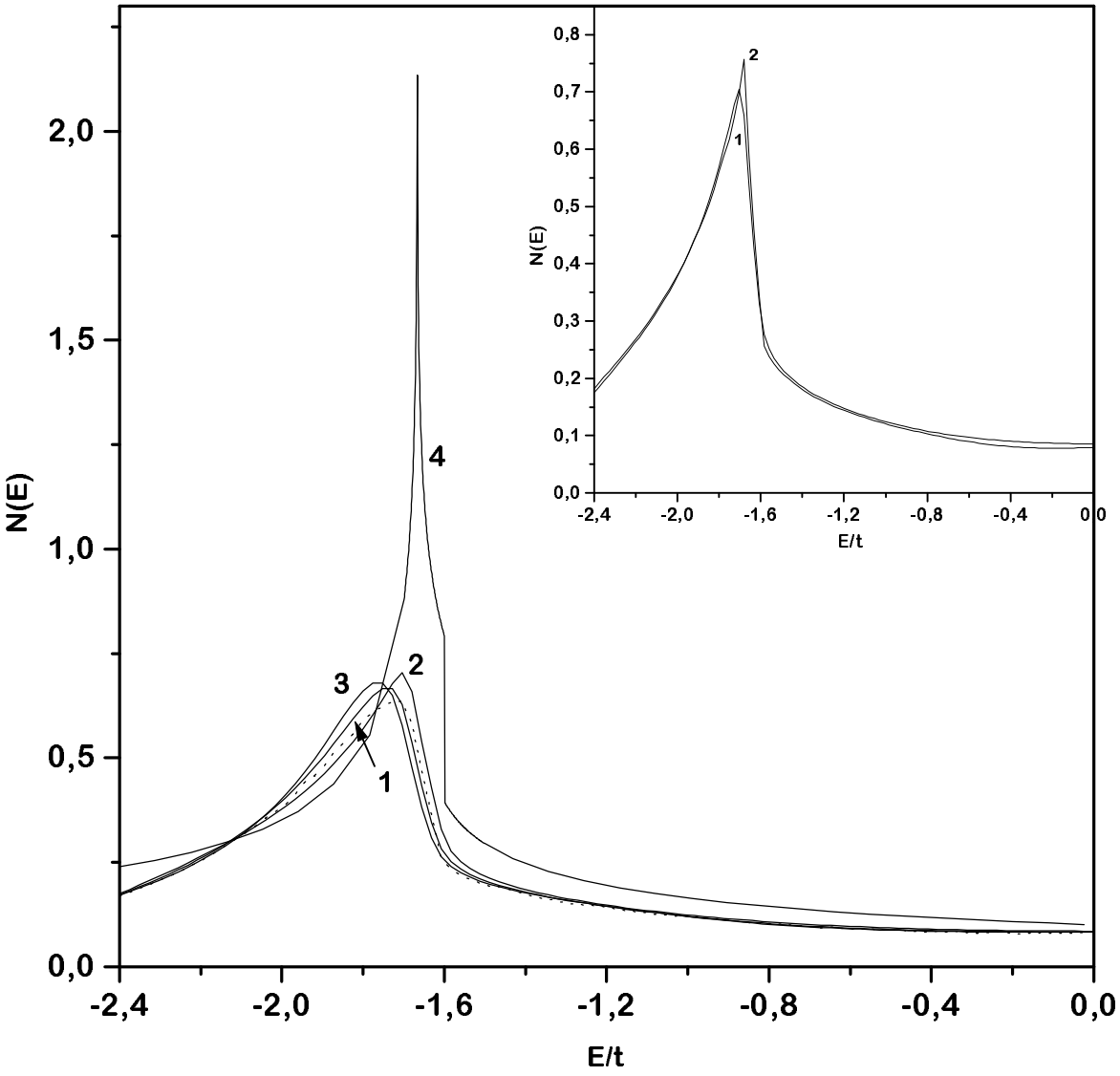

Fig.9(b)

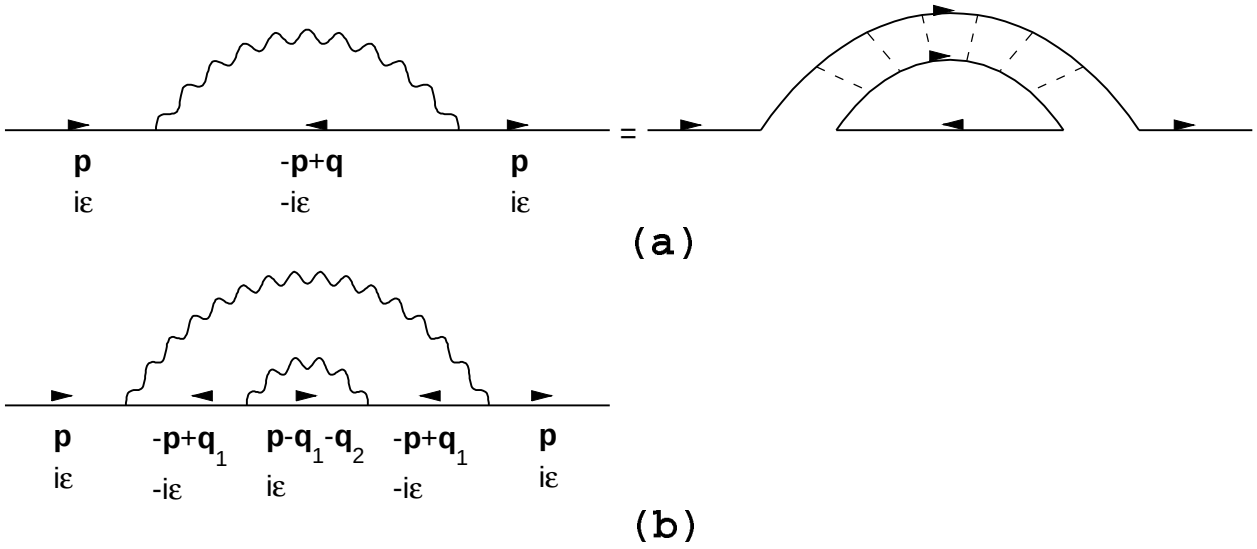

Fig.10

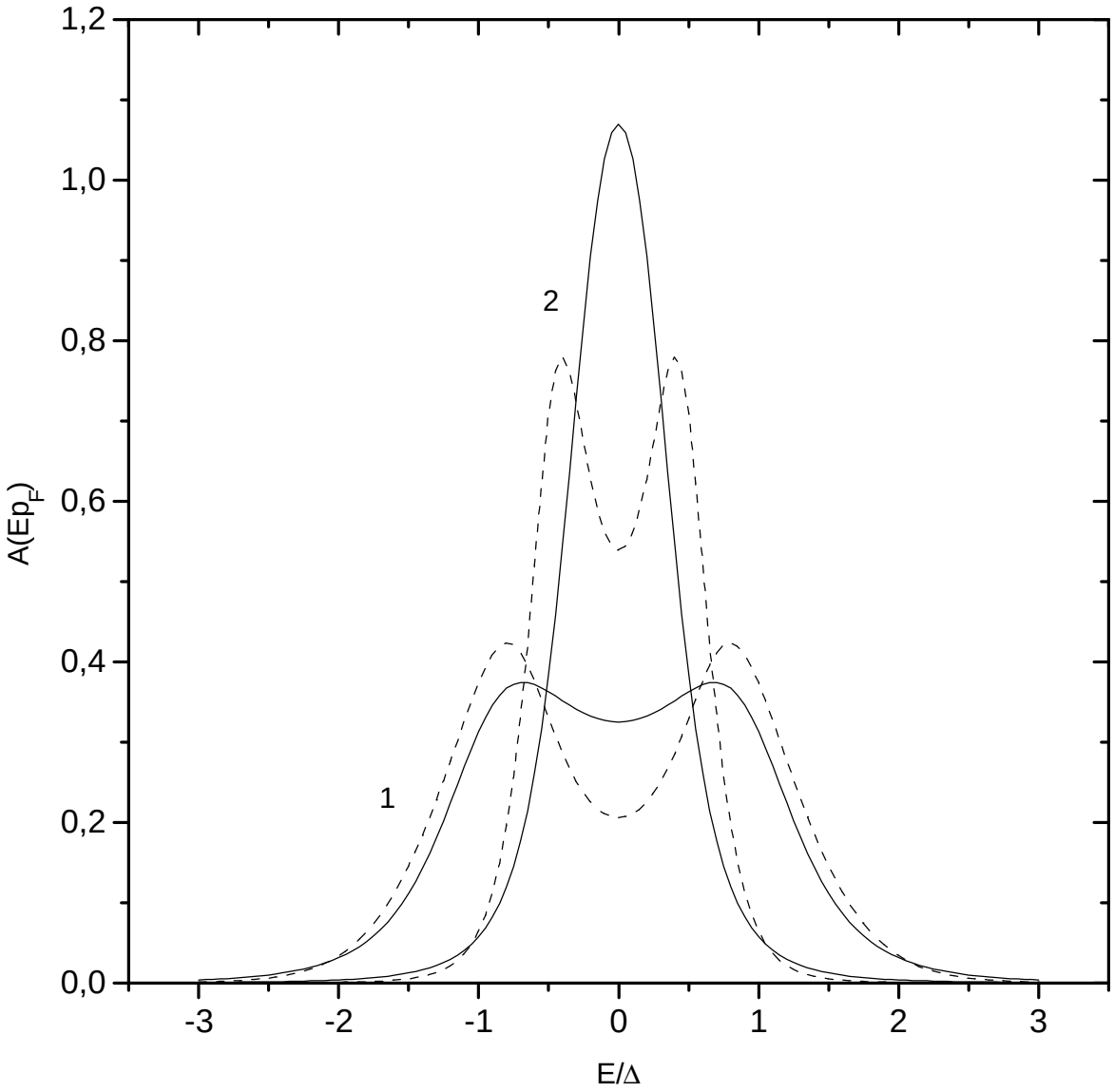

Fig.11(a)

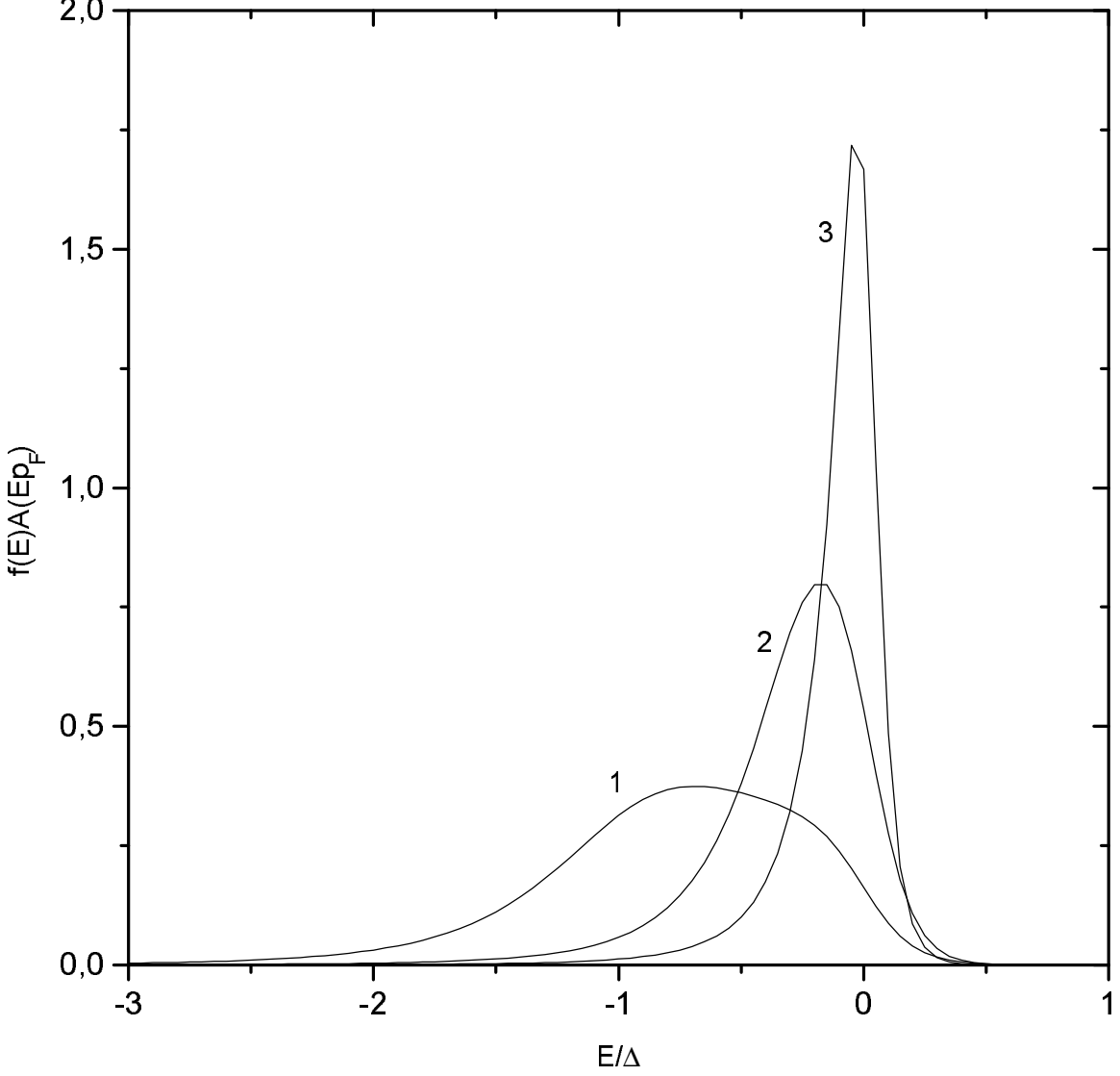

Fig.11(b)

(π,0)
(π,π)

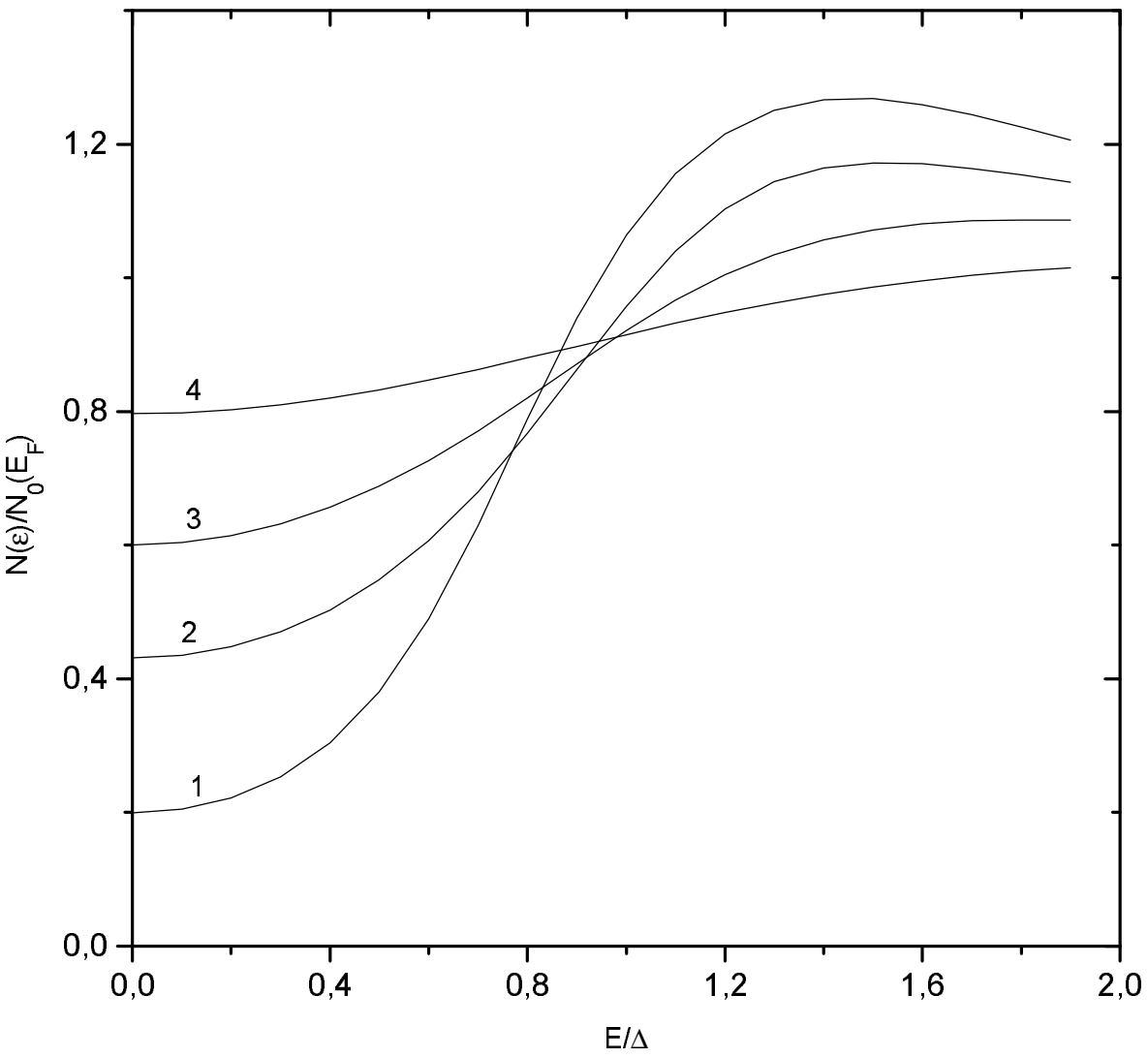

Fig.13(a)

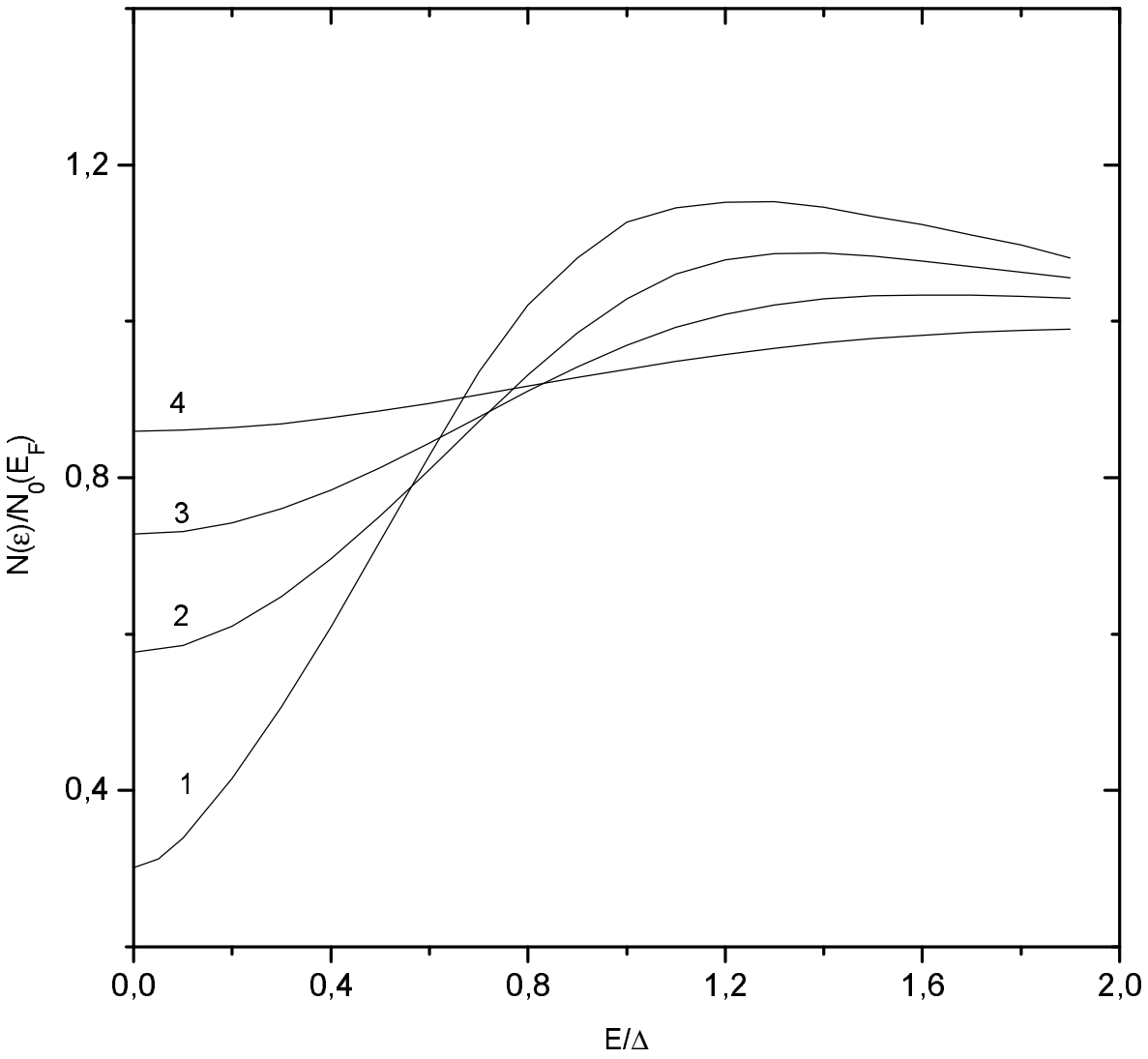

Fig.13(b)

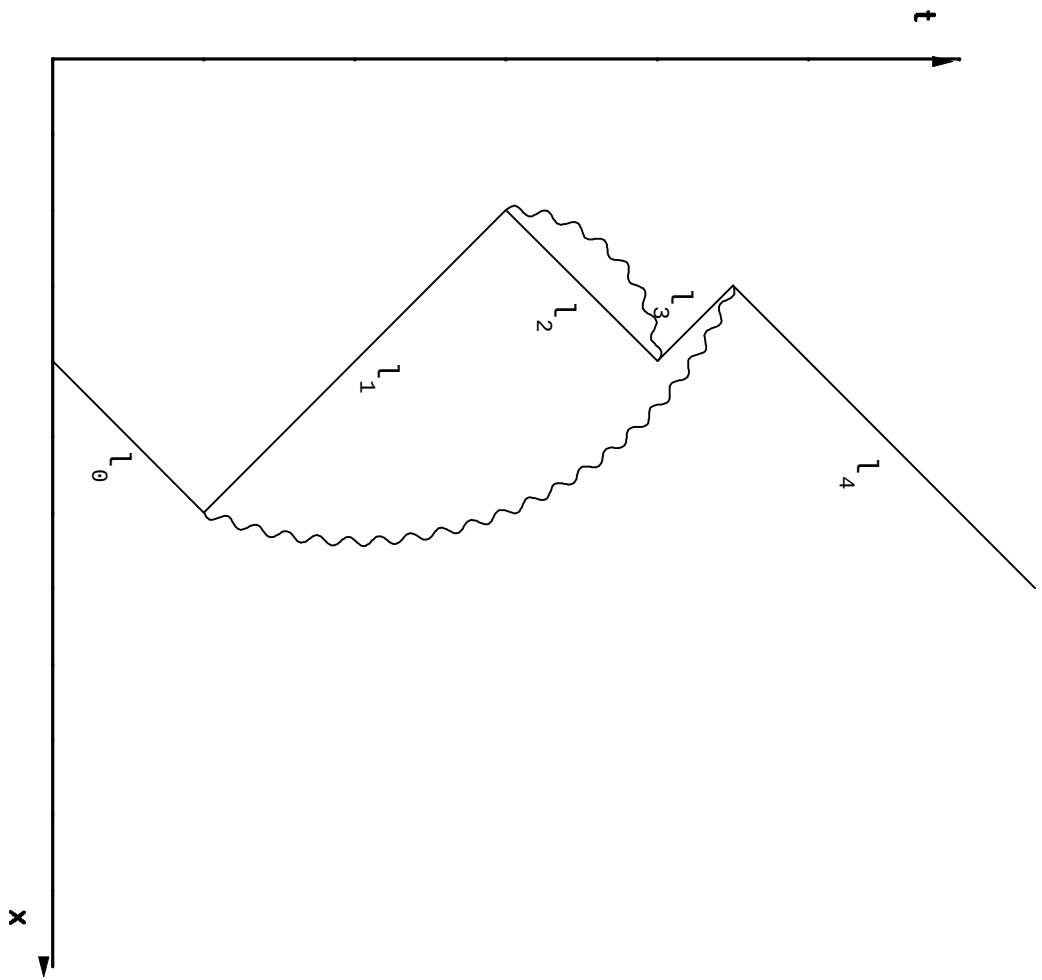

Fig.14

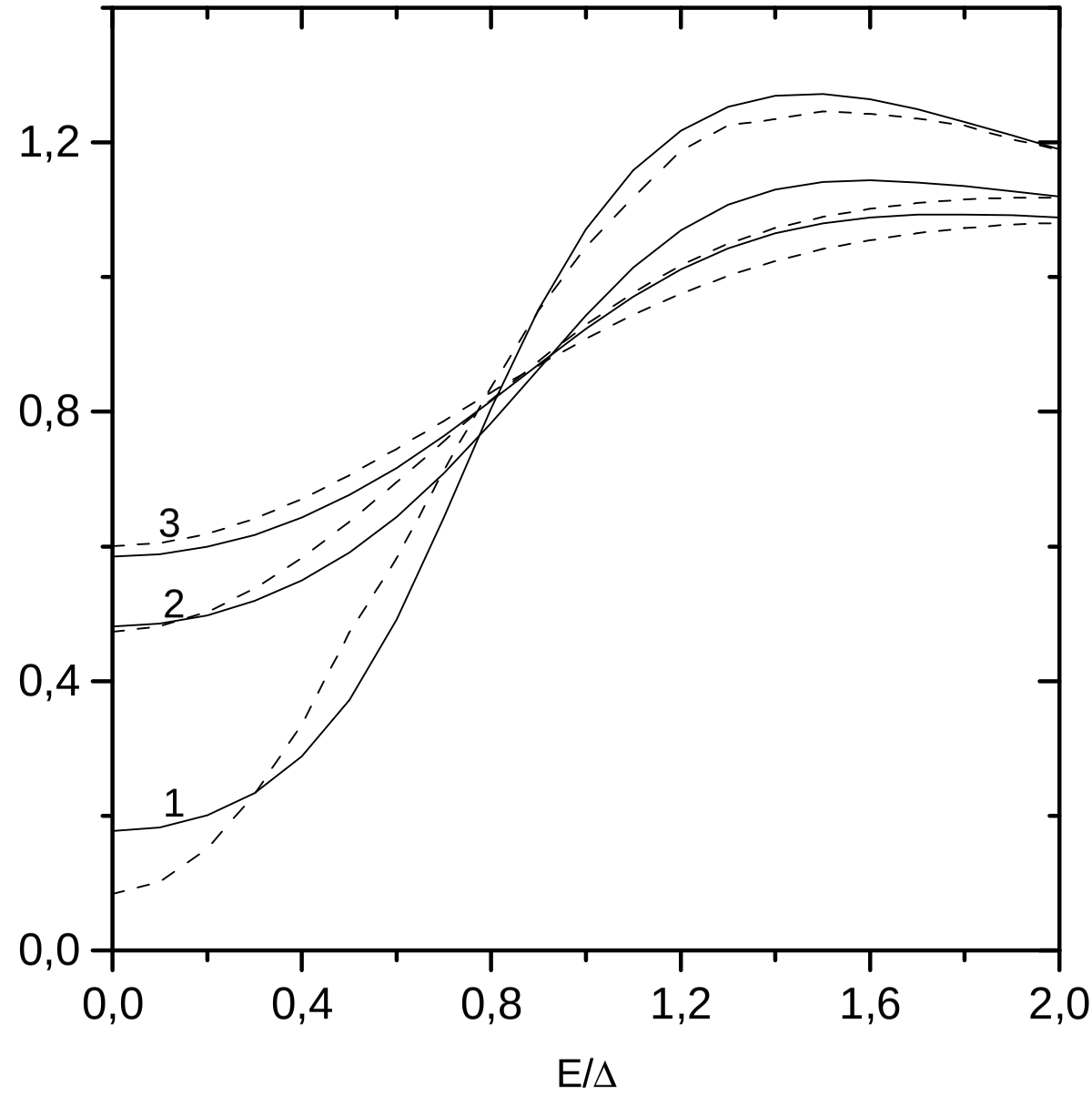

Fig.15